RNA Sequencing-Based Single Sample Predictors of Molecular Subtype and Risk of Recurrence for Clinical Assessment of Early-Stage Breast Cancer

Johan Staaf[1,*], Jari Häkkinen[1], Cecilia Hegardt[1], Lao H Saal[1], Siker Kimbung[1], Ingrid Hedenfalk[1], Tonje Lien[2,3], Therese Sørlie[2,4], Bjørn Naume[4,5], Hege Russnes[2,3], Rachel Marcone[6,7], Ayyakkannu Ayyanan[6], Cathrin Brisken[6], Rebecka R. Malterling[8], Bengt Asking[8], Helena Olofsson[9, 10], Henrik Lindman[11], Pär-Ola Bendahl[1], Anna Ehinger[1,12], Christer Larsson[13], Niklas Loman[1,14], Lisa Rydén[15,16], Martin Malmberg[14], Åke Borg[1] and Johan Vallon-Christersson[1,*]

[1]Division of Oncology, Department of Clinical Sciences Lund, Lund University, Medicon Village, SE 22381 Lund, Sweden
[2]Department of Cancer Genetics, Institute for Cancer Research, Oslo University Hospital, POB 4953 Nydalen N-0424, Oslo, Norway
[3]Department of Pathology, Oslo University Hospital, POB 4953 Nydalen N-0424, Oslo, Norway
[4]Institute for Clinical Medicine, Faculty of Medicine, University of Oslo, Oslo, Norway
[5]Department of Oncology, Division of Cancer Medicine, Oslo University Hospital, POB 4953 Nydalen N-0424, Oslo, Norway
[6]ISREC-Swiss Institute for Experimental Cancer Research, School of Life Sciences, Ecole Polytechnique Fédérale de Lausanne, CH-1015 Lausanne, Switzerland
[7]Swiss Institute of Bioinformatics, School of Life Sciences, Ecole Polytechnique Fédérale de Lausanne, CH-1005 Lausanne, Switzerland
[8]Department of Surgery, Region Jönköping County, Jönköping, Sweden
[9]Department of Clinical Pathology, Akademiska hospital, Uppsala, Sweden
[10]Department of Pathology, Centre for Clinical Research of Uppsala University, Vastmanland´s Hospital Västeras, Sweden
[11]Department of Immunology, Genetics and Pathology, Uppsala University Hospital, Uppsala, Sweden
[12]Department of Genetics and Pathology, Laboratory Medicine, Region Skåne, Lund, Sweden
[13]Division of Translational Cancer Research, Department of Laboratory Medicine, Lund University, Lund, Sweden
[14]Department of Hematology, Oncology and Radiation Physics, Skåne University Hospital
[15]Division of Surgery, Department of Clinical Sciences, Lund University, Lund, Sweden
[16]Department of Surgery and Gastroenterology, Skåne University Hospital Malmö

*** Corresponding authors:**
Johan Vallon-Christersson
Division of Oncology, Department of Clinical Sciences Lund, Lund University, Medicon Village, SE-22381 Lund, Sweden
johan.vallon-christersson@med.lu.se
Phone: +46462220383
Fax: +4646147327

Johan Staaf
Division of Oncology, Department of Clinical Sciences Lund, Lund University, Medicon Village, SE-22381 Lund, Sweden
johan.staaf@med.lu.se
Phone: +46462221444
Fax: +4646147327

ABSTRACT

Background

Multigene expression assays for molecular subtypes and biomarkers can aid clinical management of early breast cancer. Based on RNA-sequencing we aimed to develop robust single-sample predictor (SSP) models for conventional clinical markers as well as molecular intrinsic subtype and risk of recurrence (ROR) that provide clinically relevant prognostic stratification.

Methods

A uniformly accrued breast cancer cohort of 7743 patients with RNA-sequencing data from fresh tissue was divided into a training set (n=5250) and a reserved test set (n=2412). We trained SSPs for PAM50 molecular subtypes and ROR assigned by nearest-centroid (NC) methods and SSPs for conventional clinical markers from histopathology data. Additionally, SSP classifications were compared with Prosigna in two external clinical series (ABiM, n=100 and OSLO2-EMIT0, n=103 cases).

Results

In the test set, agreement between SSP and NC classifications for PAM50 (five subtypes) and Subtype (four subtypes) was high (85%, Kappa=0.78) and very high (90%, Kappa=0.84) respectively. Accuracy for ROR risk category was high (84%, Kappa=0.75, weighted Kappa=0.90). The prognostic value for SSP and NC classification was assessed as equivalent and added clinically relevant prognostic information. Agreement for SSP and histopathology was very high or high for receptor status, while moderate and poor for Ki67 status and Nottingham histological grade (NHG), respectively. SSP concordance with Prosigna was high for subtype (OSLO=83% and ABiM=80%, Kappa=0.73 and 0.72, respectively) and moderate and high for ROR risk category (68% and 84%, Kappa=0.50 and 0.70, weighted Kappa=0.70 and 0.78). In pooled analysis, concordance between SSP and Prosigna for emulated treatment recommendation dichotomized for chemotherapy (yes vs. no) was high (85%, Kappa=0.66). In postmenopausal ER+/HER2-/N0 patients SSP application suggested changed treatment recommendations for up to 17% of patients, with nearly balanced escalation and de-escalation of therapy.

Conclusions

Robust SSP models, mimicking histopathological variables, PAM50, and ROR classifications can be derived from RNA-sequencing that closely matches clinical tests. Agreement and outcome analyses suggest that NC and SSP models are interchangeable on a group-level and nearly so on a patient level. Retrospective evaluation in ER+/HER2-/N0 early breast cancer suggested that molecular testing could lead to a changed therapy recommendation for about one-fifth of patients.

Introduction

The majority of women with early-stage invasive breast cancer (IBC) are candidates for adjuvant systemic treatment. Prognosis and treatment decisions are routinely based on menopausal status, disease burden, Nottingham histological grade (NHG) and immunohistochemical (IHC) measurements of estrogen receptor (ER), progesterone receptor (PR), human epidermal growth factor receptor 2 (HER2), and the proliferation marker protein Ki67, as well as the copy number of HER2 assessed by *in situ* hybridization [1]. Diverse prognosis and unpredictable benefits of adjuvant treatment are prominent in the large ER+/HER2- luminal subgroups of breast cancer (BC). Here, overtreatment remains a major clinical challenge, a cause of decreased quality of life, and a high economic burden for the individual and society.

Multigene expression assays have in the past decades been demonstrated to provide guidance in the selection of patients with luminal disease for adjuvant chemotherapy in addition to endocrine treatment, especially in postmenopausal patients [2-4]. Whereas most multigene signatures are developed by the public research community, clinical use has largely been restricted to commercial implementations of individual signatures using targeted assays [5]. These clinical tests are based on data from mainly retrospective analyses of different patient cohorts, but also on a few prospective clinical trials [2,6]. An important limitation of current clinical multigene tests is their targeted design, providing only a limited number (typically one) of clinically useful outputs per analysis. In this context, global mRNA sequencing (RNA-sequencing) may provide a more generic solution, but current prediction models lack validation.

One of the current targeted clinical multigene tests is the Prosigna assay, which is based on the PAM50 molecular subtype classification [7], omitting the Normal-like subtype, and implemented on the Nanostring nCounter Analysis System. Along with the PAM50 subtypes, Parker and colleagues also reported the construction of risk of recurrence (ROR) scores based on subtype correlations and a dichotomized tumor size variable [7]. The equation for ROR and risk classification cutoff was constructed using a cohort of predominantly node-negative patients not receiving adjuvant systemic therapy and with long (median 9 years) clinical follow-up, while prediction of preoperative chemotherapy sensitivity was evaluated in patients based on pathological complete response [7]. A re-engineered assay based on PAM50 classification and developed for formalin-fixed, paraffin-embedded (FFPE) tissue was subsequently implemented on the Nanostring nCounter Analysis System and validated as the clinical Prosigna test that reports four subtypes and a ROR score [8]. Since the first report of the PAM50 subtypes and ROR, the prognostic value of these classifications has repeatedly been demonstrated [9-12] and it has been shown that the Prosigna test recapitulates and matches properties of the published PAM50 classifier and ROR model [8,13].

Similar to most multigene expression models, PAM50 subtypes and ROR rely on normalization to quantify gene expression relative to a reference. New samples are assigned a class label by measuring a distance in relative gene expression space to class centroids and selecting the nearest one, i.e., nearest-centroid (NC) classification. In order for the distance measure to be valid, new samples must be normalized to appropriately adjust their gene expression in relation to the used reference centroids. Failure to do so can result in erroneous classification [8,14-17] but when performed correctly classifications are valid [8]. One strategy is to use a fixed and standardized normalization of every new sample to be classified. However, this requires the use of a uniform platform consistent over time, which might be challenging, and methods reliant on data transformations derived from other samples are not considered true single-sample predictors.

An alternative strategy involves models built on rules that only consider gene expression values from a single sample, independent of normalization to reference samples and was suggested for absolute assignment of breast cancer intrinsic molecular subtype (AIMS) by Paquet and Hallett [14]. Such models are built by identifying a small set, e.g., <50, of gene-pair rules specific for the respective class and based on the form: expression of gene A > expression of gene B. New samples are classified by evaluating these gene-pair rules and assigning a class by the largest number of fulfilled rules or by a probability model [14,18]. Such models can rightfully be termed single-sample predictors (SSPs) and have been shown to be applicable for cancer classification problems including distinct molecular subtypes [14,19] as well as for continuous variables such as cell proliferation signal [19]. Even though SSP models have features attractive for clinical implementation, robust implementations relevant for BC diagnostics and treatment decision support are still lacking.

In the present study we aimed to develop and benchmark RNA-sequencing based SSP models for conventional clinical BC biomarkers, the four intrinsic molecular subtypes corresponding to Prosigna subtypes, and ROR scores. To construct and evaluate SSPs we used a uniformly accrued population-based cohort of BC comprising 7868 patients from South Sweden analyzed by whole transcriptome RNA-sequencing (>19000 genes) through the Swedish Cancerome Analysis Network - Breast (SCAN-B, ClinicalTrials.gov ID NCT02306096) study [20-22]. This unique cohort allows generalization and real-world side-by-side prognostic assessment of developed predictors in clinically relevant subgroups with available follow-up data. Moreover, retrospective analysis enables estimation of the possible impact on

therapy recommendations from SSP-based molecular subtype and ROR in the clinical decision-making. Finally, we performed benchmarking of our developed SSPs against the Prosigna test in two smaller independent clinical series. Taken together, we demonstrate that appropriate sampling of fresh BC tissue, i.e., not FFPE, can be effectively integrated into current clinical routine practices and used for cost effective RNA-sequencing with different SSPs for expression-based diagnostic and prognostic purposes. Thus, our study moves the usefulness and role of RNA-sequencing one step closer towards clinical implementation.

Material and Methods

Ethics approval and informed consent

All SCAN-B and ABiM enrolled patients provided written informed consent prior to study inclusion. The included ABiM cohort is from patients enrolled in the population-based All Breast Cancer in Malmö study and data is available on line as described [24]. Ethical approval was given for the SCAN-B study (approval numbers 2009/658, 2010/383, 2012/58, 2013/459 and 2015/277) and ethical approval was given for the ABiM study (approval number 2007/155) by the Regional Ethical Review Board in Lund, Sweden, governed by the Swedish Ethical Review Authority, Box 2110, 750 02 Uppsala, Sweden. Included normal breast tissue was obtained from women undergoing mammoplasty surgery with no previous history of BC, who gave informed consent, and the tissue samples were examined by the pathologist to be free of malignancy and processed as described [23]. The study was approved by the Cantonal ethics committee, Commission Cantonale d'éthique de la recherche sur l'être humain, CER-VD, Avenue de Chailly, 1012 Lausanne, Switzerland (Approval number 183/10). The included OSLO2-EMIT0 breast cancer cohort is from OSLO2, a prospective observational study that enrolled BC patients with primary operable disease at hospitals in southeastern Norway between 2015 and 2020. Informed consent was obtained from all patients included in the OSLO2 study. Ethical approval was given for the OSLO2 study (approval number 29668) by the Norwegian South-East Regional Committee for Medical and Health Research Ethics, Postboks 1130, Blindern, 0318 Oslo, Norway.

Patient material

Included patient cohorts are outlined in Figure 1a. The SCAN-B material comprises a population-based consecutively enrolled series of BC patients accrued at seven hospitals in the south Sweden health care region, and at two additional Swedish hospitals (Jönköping and Uppsala). Patient management, including adjuvant systemic and radiotherapy treatment have been performed according to national and regional treatment guidelines at the time of enrollment. SCAN-B patients included in this study were enrolled between September 1 2010 and May 31 2018 and sample collection and work-up followed reported SCAN-B procedures and protocols [20,22]. Clinicopathological and follow-up data as well as information on adjuvant medical treatment was obtained from the Swedish National Quality Register for Breast Cancer (NKBC [25]). Clinicopathological data reported to NKBC was determined by each respective local pathology department and according to current Swedish clinical guidelines and definitions. For details on pathological assessment see KVAST documents published by the Swedish society of Pathologists (Svensk förening för Patologi - KVAST - document [26]. For the earlier part of the material (2010-2014), characteristics of the enrolled patients, collected samples, and RNA-sequencing data has previously been shown to represent the BC population in the recruitment region [20-22,27]. Available data on adjuvant therapy for the SCAN-B cohort include dichotomized status for systemic endocrine, chemotherapy and HER2-directed therapy. The indication for adjuvant therapy in patients with ER+/HER2- tumors is regularly updated and documented in the Swedish national treatment guidelines.

The external OSLO2-EMIT0 cohort is a population-based consecutive clinical series of early BC patients accrued during 2015 and 2016 as part of the OSLO2 study [28]. The external ABiM cohort is a consecutive clinical series of patients with preoperative diagnosis of IBC scheduled for surgery in Malmö, Sweden, during the years 2007–2009 [29]. For the OSLO2 and ABiM material, freshly collected, macroscopically evaluated, and snap frozen tumor tissue was obtained by clinical pathologists at pathology departments as described [29,30] and total RNA was extracted similar to SCAN-B cases. Consensus scoring for the ABiM material from histopathology reassessment has previously been performed as described by Brueffer et al. [24].

Gene expression analysis

RNA-sequencing was performed as described [20] or by Illumina stranded TruSeq mRNA protocol, either implemented on KingFisher or on the Illumina NeoPrep system. Expression data (Fragments Per Kilobase per Million reads, FPKM) from stringtie was derived from RNA-sequencing data using an analysis pipeline to align and estimate gene expression values for sequenced samples. The RNA-sequencing analysis pipeline is based on a collection of open source software tools; picard tools [31], trimmomatic [32], bowtie2 [33], hisat2 [34,35], stringtie [36] with the GRCh38 human genome primary assembly, dbSNP [37], and GENCODE [38] transcriptome model as detailed in Supplemental methods. Entrez ID from the Gencode27 metadata was used as gene identifiers.

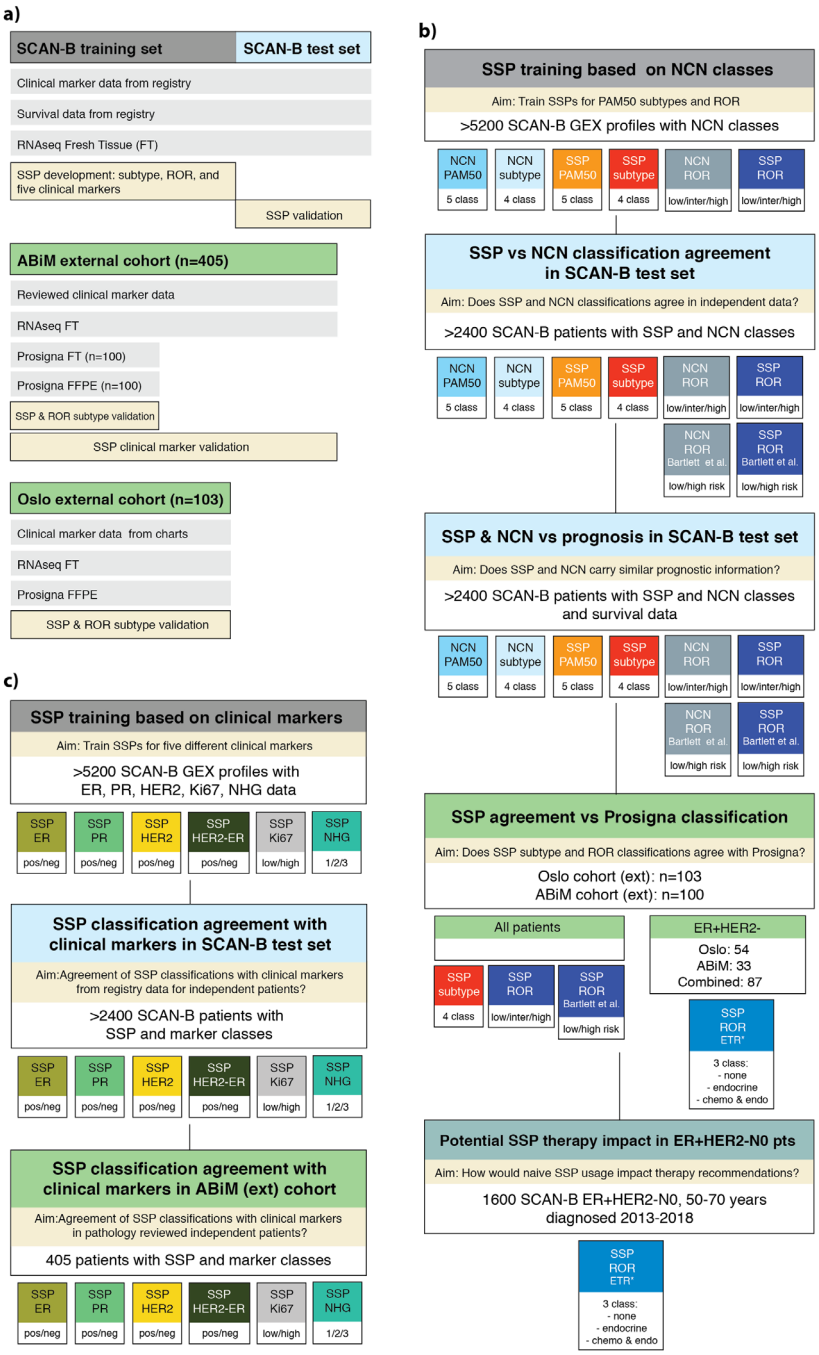

Figure 1. Outline of the study. (a) Study cohorts: SCAN-B, ABiM, and OSLO2-EMIT0. Available data types and usage outlined. FT: fresh tissue. **(b)** Scheme for development and validation of SSP models for PAM50 subtypes and ROR based on training versus NCN equivalents. Scheme outlines created SSP models and their usage in different cohorts. NCN and SSP 4-class subtype models include Basal-like, HER2-enriched, Luminal A and Luminal B subtypes. Binary SSP-ROR and NCN-ROR risk classes were created similar as described by Bartlett et al. [5]. An emulated 3-group SSP-ROR treatment recommendation (SSP-ROR-ETR) was created based on published Norwegian guidelines for Prosigna usage and applied to relevant SCAN-B patients based on guidelines. **(c)** Scheme for development and validation of SSPs for clinical markers: ER, PR, HER2, Ki67, and NHG. Scheme outlines created SSP models and their usage in different cohorts.

Assigning PAM50 subtype and ROR score using nearest centroid

PAM50 subtype and ROR score were assigned by NC classification following a general and established strategy previously described [7]. This strategy requires an appropriate static reference set to use for normalization before calculating correlations to the published PAM50 centroids. In order to correctly transform gene expression we selected a static reference set by matching the clinicopathological metadata of the training population

from which the centroids were derived [7]. Moreover, our large dataset permitted us to advance the NC strategy by selecting multiple reference sets, thereby avoiding relying on a single selection. Therefore, the selection procedure was repeated 100 times to create a series of individual static reference sets, each mimicking the original training population. The collection of reference sets was used to construct an extended NC classifier, i.e., a NC classifier utilizing 100 separate normalizations. Herein we refer to this extended NC classifier as NCN. Using multiple reference sets for normalization makes it possible to account for heterogeneity that prevails even within the restricted boundaries set by the target population. Subtype assignment from NCN was done by majority vote whereas ROR score from NCN was calculated using the average of 100 scores, each calculated as described [3] (Supplemental methods).

Training SSP models using the AIMS procedure

For training SSP models with the described AIMS method [14] we used scripts available from the AIMS GitHub repository [39]. Training was largely performed as described by Paquet et al.[14] but using gene expression data for >19000 genes, a 5-fold cross-validation repeated five times, and evaluating up to 50 selected gene-pair rules. We used weighted rule selection to adjust for differences in size between subsets of data from different library protocols. Evaluation of parameters used was strictly limited to a subset of the training cohort. To this end, the training cohort was partitioned into provisional training/evaluation sets. However, the final training was performed using the full training cohort that, importantly, had no overlap with our reserved test set. Input gene expression in both training and subsequent validations was untransformed expression values as outputted by stringtie for all protein-coding genes from Gencode27 annotated with Entrez ID. Positive controls for normal breast tissue were omitted from all SSP training. Details of the training are outlined in Supplemental methods.

Prosigna classification

Prosigna results were obtained from FFPE tumor tissue sections from clinical routine procedures as prescribed for the Prosigna assay (Prosigna insert 2017-07 LBL-C0191-09). For the OSLO2-EMIT0 material, the Prosigna assay was run at the local pathology department using the clinical Prosigna assay on the nCounter instrument in Dx mode. For the ABiM material, the Nanostring gene expression data was generated at the Division of Oncology, Lund University using an appropriate code-set, including the genes for the Prosigna assay, and then sent to Nanostring for readout of Prosigna classification results. In addition, for the ABiM material, paired Nanostring gene expression data and readout of classification results by Prosigna models was also obtained from the RNA extracted from fresh macro-dissected tumor tissue used for RNA-sequencing (Figure 1a).

Survival analysis

Survival analyses were performed in R version 3.6.1 using the survival package with breast cancer-free interval (BCFi) as endpoint (Supplemental methods and [40] and [41] for cause of death registry). Survival curves were estimated using the Kaplan-Meier method and compared using the log-rank test. Hazard ratios were calculated through univariable or multivariable Cox regression using the coxph R function. In multivariable analyses, tumor size, patient age at diagnosis, lymph node status (positive/negative), and NHG were included as covariates when appropriate. The follow-up for outcome analyses for the evaluation of prognosis stratified for molecular subtype in the test set of early-stage IBC included 2412 patients with a median follow-up of 5.4 years (0.4-7.5). Analysis for the evaluation of prognosis stratified for ROR and molecular subtype in the test set of early-stage postmenopausal ER+/HER2-/N0 IBC included 773 patients with a median follow-up of 5.6 (0.4-7.3).

Data availability statement

Gene expression data will be available through Gene Expression Omnibus (GEO) upon acceptance. Clinicopathological data and a complete list of classifications for samples will be available as Supplementary Data Table 1.

Results

Study cohorts

During the inclusion period, 11790 patients provided an informed SCAN-B consent based on either a diagnosis of BC or a suspected BC. In the current study, we included 7743 enrolled patients, based on availability of tissue and RNA-sequencing data, with a total of 8350 gene expression profiles (GEXs) generated from obtained tissue specimens as described [22] (including GEXs from bilateral diagnoses, multiple patient specimens, and repeated RNA-sequencing experiments). We assigned these patients to three partly overlapping cohorts as shown in Table 1 and Supplemental Figure 1a: i) a training set agnostic to variables other than available GEX in order to maximize training size for SSP models, i.e., including for instance multiple GEX profiles per patient and irrespective of verified BC or suspected BC diagnosis, ii) a test set with 2412 early-stage IBC patients, and iii) a larger cohort with 6660 IBC patients, referred to as the early-stage follow-up cohort hereon. As shown in Supplemental Figure 1a, the 6660-patient early-stage follow-up cohort overlapped with both the

Table 1. Study material characteristics and clinicopathological variables for SCAN-B.

	Early stage follow-up cohort[a]		Test set[b]		Training set[c]	
	Number	**%**	**Number**	**%**	**Number**	**%**
Patients	6660	-	2412	-	5250	-
Cases	-	-	-	-	5341	-
Samples	-	-	-	-	5711	-
GEX	-	-	-	-	5857	-
OAS						
Median[d] (range[d]) Follow Up Years	3.6 (0.1-7.8)	-	6.0 (1.1-7.8)	-	2.5 (0.1-8.5)	-
Events	503	7.6	278	11.5	340	6.3
Unknown	2		0		426	
BFCi						
Median[d] (range[d]) Follow Up Years	3.5 (0.2-7.8)	-	5.4 (0.4-7.5)	-	2.5 (0.2-8.0)	-
Events	306	5.1	185	7.7	198	4.4
Unknown	691		1		1362	
Age at diagnosis						
Median (range)	65 (25-95)	-	65 (25-95)	-	65 (25-95)	-
≤50	1373	20.6	499	20.7	1178	21.7
>50	5287	79.4	1913	79.3	4255	78.3
Unknown	0		0		424	
ER Status						
Positive	5678	85.7	2073	86	4367	84.6
Negative	946	14.3	337	14	792	15.4
Unknown	36		2		698	
PR Status						
Positive	4714	71.2	1764	73.2	3568	69.2
Negative	1908	28.8	645	26.8	1588	30.8
Unknown	38		3		701	
Node Status						
Positive	2310	35.5	877	36.7	1800	36.1
Negative	4194	64.5	1514	63.3	3184	63.9
Unknown	156		21		873	
HER2 Status						
Positive	801	12.6	278	11.6	636	13.6
Negative	5571	87.4	2122	88.4	4051	86.4
Unknown	288		12		1170	
Tumor Size (mm)						
Median (range)	17 (0-250)	-	20 (0-115)	-	21 (0-250)	-
≤10 mm	952	14.6	311	13	738	15.1
>10 ≤20 mm	3382	51.8	1249	52.3	2445	50.2
>20 mm	2196	33.6	830	34.7	1689	34.7
Unknown	130		22		985	
Grade						
1	1026	16.1	369	15.7	752	15.9
2	3185	50.1	1159	49.2	2387	50.3
3	2152	33.8	829	35.2	1602	33.8
Unknown	297		55		1116	
Histological type						
Ductal	5177	78	1936	80.5	3950	76.6
Lobular	917	13.8	311	12.9	733	14.2
Ductal/Lobular mixed	128	1.9	32	1.3	120	2.3
Other	415	6.3	126	5.2	357	6.9
Unknown	23		7		697	
Clinical Subgroup						
ER+/HER2-/N0	3197	50	1207	50.3	2279	47.7
ER+/HER2-/N+	1727	27	666	27.8	1309	27.4
HER2+/ER-	254	4	85	3.5	221	4.6
HER2+/ER+	564	8.8	193	8	462	9.7
TNBC	649	10.2	248	10.3	509	10.6
Unknown	269		13		1077	
Clinical Subgroup						
ER+/HER2-/N0/Age>50	2663	41.3	1008	41.9	1890	38.3
ER+/HER2-/N+/Age>50	1333	20.7	521	21.7	1001	20.3
Other	2456	38.1	877	36.5	2044	41.4
Unknown	208		6		922	

[a]The early-stage follow-up cohort have no patient redundancy, i.e., contain one GEX profile per patient.

[b]The test set is a subset fully within the early-stage follow-up cohort. There is no overlap between the test set and training set.

[c]Part of the training set overlap with the early-stage follow-up cohort. Statistics for the training set are summarized on GEX.

[d]Median and range calculated for patients without event.

training set (partial overlap) and the test set, while the test set is completely independent from the training set. The early-stage follow-up cohort and hence the test set are non-redundant, i.e., included patients are represented by only one GEX profile. The reason for creation of the 6660-patient cohort (using clinical data obtained from the NKBC as outlined in Supplemental Figure 1b) was to form a cohort representative of the underlying background population of the catchment area of the SCAN-B study in Sweden (Supplemental Figure 1c). Based on the early-stage follow-up cohort we could define a suitable independent test set for validation, prioritizing long follow-up by selecting patients diagnosed between 2010-2013 (median of 5.4 years for BCFi). In addition, the 6660-cohort also allowed us to naively assess the potential impact of SSP classification on treatment recommendations in a population representative manner. The usage of the different SCAN-B derived data subsets as well as external validation datasets is schematically shown in Figure 1a.

Training SSP models for molecular subtypes of breast cancer

We trained an SSP model for five subtypes (SSP-PAM50) on the subtype classes assigned by our NCN model (NCN-PAM50) (Figure 1b). In total, 5255 GEX profiles were used in the training: Basal-like n=552, Her2-enriched n=528, Luminal A n=2573, Luminal B n=1377, and Normal-like n=225. The maximum overall agreement was observed at 24 gene-rules per subtype (Supplemental Table 1). Only marginal improvement was observed using >15 gene pair rules, consistent with previous reports [14]. The number of unique genes (Entrez ID) represented in the selected model rules for all five subtypes was 216, of which 27 overlap with the reported PAM50 genes. The overall accuracy of SSP-PAM50 for predicting NCN-PAM50 in the training set was 85%.

An SSP model with four subtypes (SSP-Subtype) that would correspond to Prosigna subtypes was trained on NCN-Subtype labels (Figure 1b) from 5202 GEX profiles: Basal-like n=578, Her2-enriched n=529, Luminal A n=2718, and Luminal B n=1377. The maximum overall agreement in training was observed at 21 gene-rules per subtype (Supplemental Table 1), with only marginal improvement observed beyond 10 gene pair rules. The number of unique selected genes was 153, of which 27 genes overlap with PAM50 genes. The overall agreement of SSP-Subtype for predicting NCN-Subtype in the training set was 90%.

Concordance between SSP and NCN for molecular subtypes in the independent test set

SSP models for molecular subtype were validated in our reserved test set of 2412 patients (Figure 1b). Overall agreement between SSP and NCN classifications for PAM50 (five subtypes) was 85% (Kappa=0.78) (Supplemental Figure 2a and Supplemental Table 2). The agreement is equivalent to the corresponding estimate from the training set, indicating that over-fitting has not occurred, and is higher than what was reported in the original AIMS study (77%) [14]. The overall agreement for PAM50 (five subtypes) remains high (83%) even when 55 cases assigned as unclassified by NCN are regarded as discordant. For SSP-PAM50, the largest individual group of discordance is Luminal A by NCN assigned as Normal-like by SSP (128/1212 cases, 11%), consistent with findings in the original AIMS study [14]. Other similarities with the original AIMS study include groups of Luminal B and Normal-like by NCN assigned as Her2-enriched and Luminal A respectively by SSP (Supplemental Figure 2a). However, for most groups of discordant assignments, their respective fraction of the NCN defined subtype is low by comparison. Overall agreement between SSP and the original AIMS method for PAM50 subtype in our validation cohort was 74% (Kappa=0.63) and corresponding overall agreement between NCN and AIMS was 70% (Kappa=0.56). The majority of the discordance occurred between Luminal A by AIMS vs. Luminal B by SSP (41% of discordant cases) and Normal-like by AIMS vs. Luminal A by SSP (36% of discordant cases).

The agreement between SSP and NCN for Subtype (four subtypes) in the test set was 90% (Kappa=0.84) (Supplemental Figure 2b and Supplemental Table 2). Here, the largest group of discordance in absolute numbers was 52 of 1311 (4%) Luminal A by NCN assigned as Luminal B by SSP, followed by 46 of 582 (8%) Luminal B by NCN assigned as Her2-enriched by SSP (Supplemental Figure 2b). No individual group of discordant subtype assignment by SSP represented >8% of the NCN defined subtype.

Training and validation of an SSP model for ROR in breast cancer

Since ROR score is an integer value between 0-100 we used data binning with 20 equally spaced levels to transform NCN-ROR into categorical training labels for our SSP-ROR model (Supplemental methods). For training the SSP-ROR model, NCN-ROR scores from a total of 5359 GEX profiles were stratified into binned ROR labels: <5 n=100, 6-10 n=186, 11-15 n=272, 16-20 n=314, 21-25 n=324, 26-30 n=317, 31-35 n=361, 36-40 n=318, 41-45 n=311, 46-50 n=364, 51-55 n=384, 56-60 n=390, 61-65 n=411, 66-70 n=366, 71-75 n=349, 76-80 n=272, 81-85 n=196, 86-90 n=124 profiles. The maximum overall agreement in training was observed at 21 gene-rules per subtype (Supplemental Table 1) with only marginal improvements observed using >10 gene pair rules. The union of unique genes represented in selected rules for all ROR bins was 296 of which 18 genes overlapping with the PAM50 genes. The overall accuracy in the training set for categorical binned ROR

labels was 17%. A strong linear relationship was observed between the SSP and NCN categorical value (R^2=0.87).

In the test set, overall agreement for binned NCN-ROR score and predicted SSP-ROR was 17% (Kappa=0.13, weighted Kappa=0.90), equivalent to training results. Similar to the training set, a strong linear relationship with binned ROR score (R^2=0.88) was also observed in the test set (Supplemental Figure 2c). The relationship was also visualized by boxplots of the non-binned NCN-ROR scores for SSP-ROR (Supplemental Figure 2d). Importantly, when stratified by SSP-PAM50 the distributions of ROR showed similar relationships between subtypes for NCN-ROR scores (Supplemental Figure 2e) and SSP-ROR score (Supplemental Figure 2f). Also, the distributions were as expected lower in Luminal A cases [7,8]. Distributions of ROR scores stratified by SSP-Subtype were also specifically investigated for Luminal A and Luminal B cases within the clinical subgroup of ER+/HER2- tumors (Supplemental Figure 2g-h), again finding relationships between subtypes to be similar and also consistent with what has been reported for the Prosigna assay ([8] and Prosigna insert 2017-07 LBL-C0191-09 section 15.1 Figure 9).

SSP and NCN concordance for ROR score was also investigated after relevant stratification into ROR risk category groups (Low, Intermediate, High) using cutoffs specific for nodal status [3] and used by Prosigna ([8,42] and Prosigna insert 2017-07 LBL-C0191-09 section 13.4, Table 9). For NCN-ROR, the score was calculated using the gross tumor size variable as described [3]. For SSP-ROR, the assigned score was adjusted with +5 for tumors >20mm to appropriately account for the effect of the gross tumor size variable and minimizing the risk of underestimating the score (Supplemental methods). Overall agreement between SSP and NCN for risk category was 84% (Kappa=0.75, weighted Kappa=0.90) (Supplemental Figure 2i). Effectively, all discordance (>99%) was observed between adjacent risk groups, explaining the high weighted Kappa, with discordance between Intermediate by NCN-ROR and either Low or High classification by SSP-ROR, comprising 40% and 33% of all discordant cases respectively. To illustrate and evaluate agreement that reflects practical clinical use we also performed a dichotomized comparison by combining Low and Intermediate risk classification into one category, similar to the study by Bartlett et al. [5] that compared different commercial multigene tests in BC. The overall agreement between SSP and NCN for this two-group ROR stratification was 92% (Kappa=0.84) (Supplemental Figure 2j).

Training and validation of SSP models for clinical markers in breast cancer

In addition to deriving SSPs for intrinsic molecular subtypes and ROR score, we also trained SSP models for five conventional clinical markers, ER, PR, HER2, Ki67, and NHG, using training labels based on clinicopathological registry data (Figure 1c). Cutoffs for ER and PR status were set to 10% or greater positive staining according to Swedish national guidelines. For HER2, in addition to a general SSP model, we also trained two separate SSP models specific for ER status using only ER+ or ER- cases respectively. For Ki67 status, a two-group model (High/Low) was trained using cutoffs for included tumors from the respective local pathology departments. The number of gene-rules per class at maximum overall agreement in training ranged from 3 for PR to 19 for ER (Supplemental Table 3). Performance was first evaluated in the independent test set (Table 2 and Supplemental Figure 3). Concordance with clinicopathological status was very high for ER (overall accuracy=96%, Kappa=0.86) and high for PR (overall accuracy=87%, Kappa=0.70) with clinically relevant positive predictive values (99% and 95%, respectively). Concordance was high for HER2 using ER-specific models (overall accuracy=92%, Kappa=0.67) and moderate for the general HER2 SSP model (overall accuracy=89%, Kappa=0.58). Overall concordance for HER2 SSP models was mainly negatively influenced by false positives for the SSP models. Correspondingly, the negative predictive values were high (98% for both the general and ER specific HER2 models). Concordance with clinicopathological status was moderate for Ki67 (overall

Table 2. SSP performance validated against clinicopathological registry data (NKBC) in the independent population-based SCAN-B test set.

		Accuracy			Kappa						
SSP model	**n**	**Accuracy**	**95% CI**	**AccuracyNull**	**Kappa**	**95% CI**	**class value**	**Sensitivity**	**Specificity**	**Pos Pred Value**	**Neg Pred Value**
ER	2410	0.96	(0.96, 0.97)	0.86	0.86	(0.83, 0.89)	Positive	0.97	0.96	0.99	0.82
PR	2409	0.87	(0.86, 0.89)	0.73	0.70	(0.67, 0.73)	Positive	0.88	0.87	0.95	0.72
HER2	2410	0.89	(0.87, 0.90)	0.88	0.58	(0.54, 0.62)	Positive	0.87	0.89	0.51	0.98
HER2 (SSP ER specific)	2410	0.92	(0.91, 0.93)	0.88	0.67	(0.62, 0.71)	Positive	0.86	0.93	0.60	0.98
Ki67	900	0.80	(0.77, 0.82)	0.57	0.59	(0.53, 0.64)	High	0.80	0.79	0.83	0.75
							Grade 1	0.81	0.72	0.35	0.95
NHG	2357	0.57	(0.55, 0.59)	0.49	0.38	(0.35, 0.40)	Grade 2	0.30	0.88	0.71	0.57
							Grade 3	0.84	0.79	0.69	0.90

accuracy=80%, Kappa=0.59), and fair for NHG (overall accuracy=57%, Kappa=0.38, weighted Kappa=0.60). For NHG, 80% of all discordance was from NHG Grade 2 (811 of in total 1012 discordant cases), stratified by SSP into Grade 1 or 3. This observation is consistent with previous studies dividing NHG Grade 2 tumors into low and high-proliferative cases [43,44]. By comparison, only a small fraction of discordant cases (58/1012, 5.7%) were misclassified from Grade 1 to 3 or vice versa reflected by substantially higher weighted agreement bordering moderate and high concordance. The negative predictive values were accordingly comparably high for both Grade 1 and Grade 3 (95% and 90%, respectively). To test whether discordant SSP stratification of clinical NHG status provided prognostic value we created Kaplan-Meier plots in the subgroup of patients with ER+/HER2- disease who only received endocrine adjuvant treatment (Supplemental Figure 4). A marked difference in BCFi was found for stratification of clinical NHG Grade 2 (Supplemental Figure 4b) but not of clinical NHG Grade 1 or 3 (Supplemental Figures 4a and c).

The quality of registry data in NKBC has been shown to be high [45]. In addition, review of medical chart data performed in subsets of the SCAN-B cohort has shown high validity of register data in general and for dichotomized treatment data in particular, e.g., yes/no for endocrine and chemotherapy treatment [27]. Even so, to further investigate if evaluated concordance for clinical markers was adversely affected by assessment against registry data we evaluated performance against consensus status from re-stains and re-evaluation done by three board-certified breast cancer pathologists in the independent ABiM material from Brueffer et al. [24]. Concordance was largely comparable with results in the SCAN-B test set. For Ki67, distributions appeared skewed using the Ki67 cut-off set at High >20%, as a large number of cases were given a re-evaluated consensus score of exactly 20% and most of these were classified as High by SSP (Supplemental Table 4 and Supplemental Figure 5).

Comparison between NCN and SSP stratifications by patient outcome

To further validate SSP subtype and ROR models against NCN stratification on a group level, we assessed prognostic value by survival analysis using registry data in the population representative test set (Figure 1b). Comparison with patient outcome is particularly relevant as it reflects the intended use of the classifications. Moreover, we reasoned that group level comparisons are relevant given the nature of the intrinsic subtypes and ROR classification with classes defined by underlying boundaries for relative correlations to centroids. As such, there are no obvious distinctions in underlying data between some classes (e.g., Luminal A vs B, or a continuous ROR score).

Outcome analysis typically requires comparisons within groups of uniformly treated patients. However, as the test set represents early-stage IBC in Sweden between 2010-2013 treated in accordance with national guidelines at the time of study inclusion the overall differences in outcome for intrinsic subtypes can be expected to reflect treatment outcome for each respective group. Therefore, we first compared outcome characteristics for molecular subtypes by Kaplan-Meier plots using BCFi in the full test set and irrespectively of clinical markers and administered treatment (Figures 2a-b). As expected, intrinsic subtypes display markedly separate outcome consistent with previous reports [7,46], despite a different clinical endpoint (BCFi). Patient outcomes are generally very good and highly similar between SSP and NCN with respect to Luminal A and Luminal B cases, with each respective group having >95% (Luminal A) and ~90% (Luminal B) event-free survival respectively irrespective of classification method and model.

We next focused on specific patient subgroups where the available commercial molecular assays in question are generally recommended for use in assisting treatment decisions. Prognostic value was first assessed for NCN and SSP-based intrinsic subtypes and for different ROR classification groups in patients >50 years with ER+/HER2-/N0 disease that only received endocrine adjuvant treatment (n=773). Hazard ratios and 95% confidence intervals were highly similar and overlapping between corresponding SSP and NCN based stratifications in univariable analysis (Figure 2c, left side), as well as in multivariable analysis with tumor size, age at diagnosis, and NHG as covariates (Figure 2c, right side). To further illustrate SSP and NCN stratifications we generated Kaplan-Meier plots showing similar outcome characteristics for stratifications by SSP and NCN for PAM50 subtype (Figure 2d), Subtype (four subtypes) (Figure 2e), ROR risk group classification (Figure 2f), and the two-group stratification according to Bartlett et al. [5] (Figure 2g).

The same tendency for outcome and similarity between SSP and NCN stratifications was also observed in patients with ER+/HER2-/N0 tumors that received adjuvant chemotherapy prior to endocrine treatment, although groups are small as shown for ROR risk classification (Supplemental Figures 6a-b). Furthermore, comparable prognostic stratification for SSP and NCN was seen in the similarly sized group of patients with ER+/HER2-/N0 tumors that received no adjuvant treatment (Supplemental Figures 6c-d). Here, the majority of tumors were classified as low risk by ROR score and reassuringly with none or very few BCFi events. Finally, the same pattern also extended to ROR stratification of node positive (N+) disease and the larger group of patients with ER+/HER2-/N+ tumors that only received adjuvant endocrine treatment (Supplemental

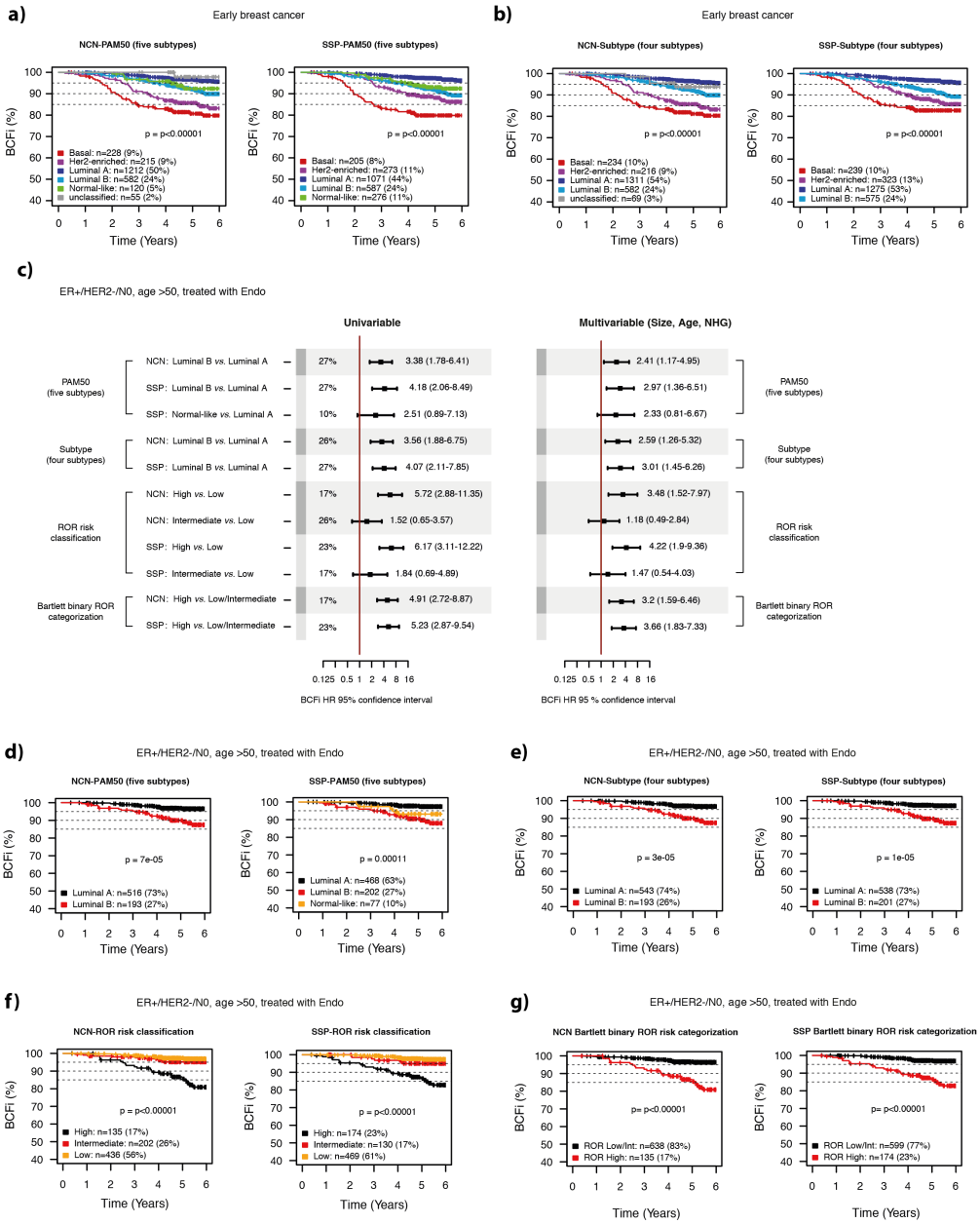

Figure 2. **Assessment of prognostic value of SSP stratification and NCN stratification.** Comparison of SSP and NCN classifications in the independent population-based test set by assessment of prognostic value. Kaplan-Maier plots for molecular subtype with five groups (PAM50) or four groups (Subtype) using BCFi as clinical end point: **(a)** PAM50 by NCN (left) and SSP (right), **(b)** Subtype by NCN (left) and SSP (right). **(c)** Cox regression analysis using BCFi as end point in the test set restricted to patients with ER+/HER2-/N0 disease diagnosed over 50 years of age that only received endocrine adjuvant treatment (n=773). Test and reference group is specified on the left. Hazard ratios and 95% confidence interval ranges from univariable analysis (left forest plot) and multivariable analysis (right forest plot) with tumor size, age at diagnosis, and NHG as covariates. Kaplan-Meier plots for stratification of ER+/HER2-/N0 disease diagnosed over 50 that only received endocrine adjuvant treatment in the test set by NCN (left in each panel) and SSP (right in each panel) for: **(d)** PAM50 subtype, **(e)** Subtype, **(f)** ROR risk classification, and **(g)** and the two-group ROR stratification according to Bartlett et al. [5].

Table 3. SSP prediction performance validated against Prosigna classification in the full external clinical series OSLO2-EMIT0 and ABiM.

OSLO2-EMIT0		Accuracy		Kappa					
SSP model vs. Prosigna*	n**	Accuracy 95% CI	AccuracyNull	Kappa 95% CI	class value	Sensitivity	Specificity	Pos Pred Value	Neg Pred Value
Subtype	103	0.83 (0.74, 0.89)	0.52	0.73 (0.62, 0.84)	Luminal A	0.85	0.90	0.90	0.85
					Luminal B	0.71	0.93	0.80	0.90
					Basal	0.86	0.99	0.92	0.98
					Her2-enriched	1.00	0.93	0.50	1.00
ROR risk classification	103	0.68 (0.58, 0.77)	0.44	0.50 (0.37, 0.63)	Low	0.74	0.86	0.65	0.90
					Intermediate	0.29	0.90	0.56	0.75
					High	0.91	0.74	0.73	0.91
Binary ROR risk categorization (Bartlett)	103	0.82 (0.73, 0.89)	0.56	0.64 (0.49, 0.78)	Low/Intermediate	0.74	0.91	0.91	0.73
					High	0.91	0.74	0.73	0.91

ABiM		Accuracy		Kappa					
SSP model vs. Prosigna^	n^^	Accuracy 95% CI	AccuracyNull	Kappa 95% CI	class value	Sensitivity	Specificity	Pos Pred Value	Neg Pred Value
Subtype	100	0.80 (0.71, 0.87)	0.38	0.72 (0.60, 0.83)	Luminal A	0.82	0.92	0.86	0.89
					Luminal B	0.74	0.86	0.74	0.86
					Basal	0.93	1.00	1.00	0.99
					Her2-enriched	0.79	0.93	0.65	0.96
ROR risk classification	98	0.84 (0.75, 0.90)	0.60	0.70 (0.57, 0.83)	Low	0.75	0.95	0.79	0.94
					Intermediate	0.58	0.95	0.73	0.90
					High	0.95	0.79	0.88	0.91
Binary ROR risk categorization (Bartlett)	98	0.89 (0.81, 0.94)	0.60	0.76 (0.63, 0.89)	Low/Intermediate	0.79	0.95	0.91	0.88
					High	0.95	0.79	0.88	0.91

*Prosigna reference is the clinical test performed on FFPE as prescribed.
**Prediction performance evaluated in OSLO2-EMIT0 (all available cases)
^Prosigna reference in ABiM is NanoString data (not clinical test) generated in Lund on FFPE material and sent to Prosigna for calculating the Subtype and ROR readout
^^Prediction performance evaluated in ABiM (all available cases)

Figures 6e-f). Within this group, about 50% of cases were categorized as either Low or Intermediate risk by ROR and contribute very few events.

Cross-comparison between SSP and Prosigna in independent external clinical series

To benchmark the developed SSP models for Subtype and ROR versus a commercially available assay, we compared classifications to results from the Prosigna assay performed on FFPE tissue in two independent external clinical series (Figure 1b): i) OSLO2-EMIT0 (n=103, clinical Prosigna assay results), and ii) ABiM (n=100, Prosigna classifications calculated from non-clinical Nanostring data). Overall accuracy Subtype assignment was 83% in OSLO2-EMIT0 and 80% in ABiM (Kappa=0.73 and 0.72, respectively) (Table 3, Supplemental Figure 7a and Supplemental Figure 8a). Overall accuracy for ROR risk category was 68% in OSLO2-EMIT0 and 84% in ABiM (Kappa=0.50 and 0.70, weighted Kappa=0.70 and 0.78, respectively). We also compared distributions of ROR score by subtype assignment in the respective full series as well as restricted to ER+/HER2- tumors classified as Luminal subtype (Supplemental Figure 7d-g and Supplemental Figure 8d-g). Concordance for two-group stratification reported by Bartlett et al. [5] was 82% in OSLO2-EMIT0 and 89% in ABiM (Kappa=0.64 and 0.76, respectively) (Table 3, Supplemental Figure 7i and Supplemental Figure 8i). In a pooled analysis of OSLO2-EMIT0 and ABiM the agreement for Subtype was 81% (Kappa=0.73), 76% for ROR risk category (Kappa=0.59, weighted Kappa=0.74), and 85% for the Bartlett two-group stratification of ROR risk (Kappa=0.70). In a pooled analysis restricted to ER+/HER2- tumors agreement for Subtype was 79% (Kappa=0.61), 75% for ROR risk (Kappa=0.61, weighted Kappa=0.74), and 86% for the Bartlett two-group stratification of ROR risk (Kappa=0.72).

Expected confounders in the above comparisons would include sampling and tissue preservation (FFPE versus fresh tissue) as noted by Nielsen et al. for the clinical Prosigna assay [42]. To assess these confounders and put concordances in a context we utilized multiple readings from different models and procurements in the ABiM cohort (Figure 1b). We first compared concordance between SSP and Prosigna using classifications from applying the respective models to data from the same RNA extract obtained from macro-dissected fresh tissue. Overall agreement for Subtype assignment increased to 87% (Kappa=0.81), in line with agreement between SSP and NCN models in the test set. Notably, ROR risk classification decreased to 79% (Kappa=0.61, weighted Kappa=0.76), whereas concordance for the Bartlett two-group risk category remained unchanged at 89% (Kappa=0.76) (Supplemental Table 5 top section). Finally, to conversely isolate the effect of sampling on discordance we evaluated agreement in the ABiM cohort solely using the Prosigna model but comparing data obtained from either FFPE tissue or from the paired macro-dissected fresh tissue. The overall agreement for Subtype assignments was 82% (Kappa 0.74), for ROR risk classification 84% (Kappa 0.71, weighted Kappa=0.84) and 90% (Kappa 0.79) with two-group categorization (Supplemental Table 5 bottom section), largely matching the agreements between SSP and Prosigna.

For a more specific comparison between SSP and Prosigna that better reflects the use for directing adjuvant chemotherapy in a clinical setting, we compared agreement for stratification that emulates treatment recommendation (ETR) in postmenopausal patients with ER+/HER2-/N0 and pT1-2 tumors adapted from Norwegian national guidelines (Supplemental methods). The ETR schema adheres to actual general recommendations but does not include individualized assessment of possible escalation or de-escalation. The treatment guidelines stratify patients into three groups with respect to recommended adjuvant treatment: None, Endo (i.e., endocrine treatment alone for 5-10 years), or ChemoEndo (i.e., adjuvant chemotherapy followed by endocrine treatment for 5-10 years). The comparison was also done for treatment recommendations dichotomized for chemotherapy, i.e., by combining None and Endo into one group. SSP performance was evaluated in both the pooled external clinical series (n=87) as well as in the respective series separately (Supplemental Table 6). Overall agreement for ETR in the pooled data was 78% (Kappa=0.65) and when dichotomized for chemotherapy was 85% (Kappa=0.66).

Assessing potential impact of SSP molecular subtype and ROR testing on use of chemotherapy

In addition to validating SSP classifications for Subtype and ROR against research-based NC classifications and benchmarking SSP against Prosigna models we also wanted to apply our SSP models in the entire 6660-patient follow-up cohort of population-based early-stage IBC (Figure 1, Table 1, Supplemental Figure 1) to assess the potential extent and type of altered treatment recommendation from using SSP models in treatment guidance. To this end we used the naïve ETR classification dichotomized for chemotherapy and compared this with information from NKBC on administered treatment.

To verify that SSP classifications were independent of year of diagnosis we first calculated the proportions of SSP-Subtype and SSP-ROR risk group in the entire population stratified by year of diagnosis. Proportions for classifications varied slightly between years but were largely stable throughout the enrollment period that extends over nine years (Figures 3a-b). Overall proportions across the entire period for SSP-Subtype were: 52% Luminal A, 25% Luminal B, 10% Basal-like and 13% Her2-enriched (Figure 3a). Corresponding proportions for SSP-ROR risk classification were: 38% Low, 15% Intermediate and 47% High (Figure 3b).

Among other clinical management indications, molecular testing is indicated for postmenopausal BC patients with ER+/HER2-/N0 with an ambiguous risk of recurrence. To attempt to represent a relevant indication we first studied patients with known treatment status diagnosed with ER+/HER2-/N0 breast cancer at age >50 years (2644/6660, 40%). In this subgroup, the use of chemotherapy differed between age groups and adjuvant therapy among the more elderly patients was largely restricted to endocrine treatment (Figure 3c). Therefore, the final clinical assessment subgroup was restricted to patients aged >50 ≤70 years to reduce the impact of high age and expected associated comorbidities as factors influencing treatment decisions. The fraction of patients receiving chemotherapy in this age-restricted subgroup increases across early years of enrollment, especially apparent from 2012, but levels out for the later years (Figure 3d). The observed increase coincides with changes in national treatment guidelines introduced during the period of enrollment. Therefore, to better extrapolate our results, estimates were calculated for patients from the later enrollment period (2013-2018). Proportions of treatment across this latter period differ to some extent from the overall and were 60% (versus 65%) with endocrine only and 24% (versus 20%) with adjuvant chemotherapy and endocrine treatment, whereas the proportion of patient that received no adjuvant treatment remained at 15% (Figure 3d). The potential effect on therapy was estimated by cross comparing the naïve ETR dichotomized for chemotherapy with NKBC records of administered systemic treatment.

In the N0 subgroup strict adherence to ETR would result in modest net increased use of adjuvant chemotherapy from 24% to 25% estimated for patients from 2013-2018 (Figure 3e). The estimated net change is the combined result from patients where treatment would be escalated with chemotherapy (No CT to CT, 9%), and patients that would be spared chemotherapy (CT to No CT, 8%). Thus, in total 17% of the investigated clinical subgroup had potential for changed chemotherapy recommendation based on SSP molecular subtyping.

In addition to estimating possible effects on therapy, we also assessed the prognostic value of the molecular test by stratification of uniformly treated subgroups. For N0 patients with no adjuvant treatment, patients suggested for endocrine treatment by SSP (50 of 219) had worse outcome (Figure 3f) with a univariable Cox hazard ratio of 7.37 (95% CI=1.35–40) (Figure 3h) and multivariable hazard ratio of 4.66 (95% CI=0.69–31) (Figure 3i). For N0 patients with endocrine therapy only, patients suggested for escalation (No CT to CT) by SSP (158 of 933) had worse outcome (Figure 3g) with a univariable Cox hazard ratio of 6.18 (95% CI=2.83–13.46) (Figure 3h) and multivariable hazard ratio of 5.01 (95% CI=2.04–12.35) (Figure 3i). For N0 patients receiving adjuvant chemotherapy the outcome is generally very good with few events and no difference in outcome for the patients suggested for de-escalation of chemotherapy by SSP classification (Figures 3h-i).

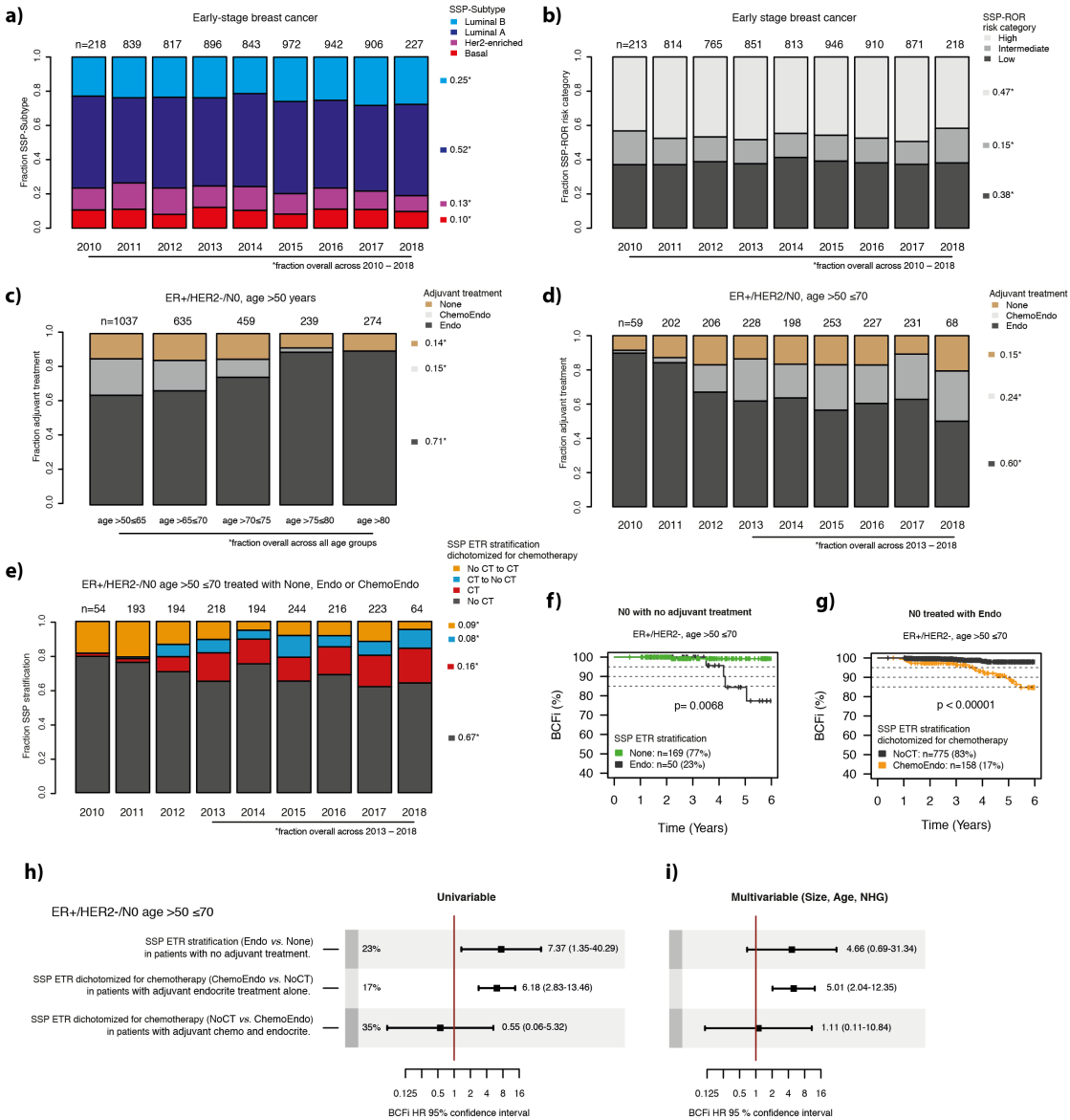

Figure 3. **SSP classifications for Subtype and ROR risk category in early-stage breast cancer and cross-comparison with administered systemic treatment.** The basis for comparisons is the 6660-patient follow-up cohort (Table 1). Summarized proportions are shown on the right side of bar graphs. The first and last year of enrollment (2010 and 2018) are not full calendar years and therefore include notably smaller numbers of enrolled patients. **(a)** Proportions of SSP-Subtype by year of diagnosis. **(b)** Proportions of SSP-ROR risk category by year of diagnosis. **(c)** Proportions for adjuvant treatment within ER+/HER2-/N0 patients diagnosed at age >50 years by different age at diagnosis. Endo: endocrine therapy only, ChemoEndo: adjuvant chemotherapy and endocrine therapy. None: no adjuvant systemic therapy. **(d)** Proportions for adjuvant treatment within ER+/HER2-/N0 patients diagnosed at age >50 ≤70 years by year of diagnosis. **(e)** Cross-comparison of the naïve SSP ETR dichotomized for chemotherapy (yes/no) with records of administered systemic treatment within ER+/HER2-/N0 patients at age >50 ≤70. The groups for which SSP treatment recommendation is in agreement with the administered treatment are shown in black for regimen without chemotherapy (No CT) and in red for regimen including chemotherapy (CT). The discordant groups where SSP would lead to escalation of treatment (No CT to CT) are shown in orange and de-escalation of treatment (CT to No CT) in blue. **(f)** Kaplan-Maier plot for SSP stratification by SSP-

ETR treatment recommendation within the N0 subgroup of ER+/HER2- patients diagnosed at age >50 ≤70 and no adjuvant treatment. **(g)** Kaplan-Maier plot for SSP stratification by SSP-ETR dichotomized for chemotherapy (chemotherapy vs. no chemotherapy) within ER+/HER2-/N0 patients diagnosed at age >50 ≤70 treated with adjuvant endocrine therapy only. **(h)** Forest plots of Hazard ratios and 95% confidence interval ranges from univariable and **(i)** multivariable Cox regression using BCFi as end point stratified using SSP treatment recommendation. Multivariable analysis is with tumor size, age at diagnosis, and NHG as covariates. Test (SSP stratification) and subgroup (administered treatment) is specified on the left of the univariable forest plot.

Discussion

In this study we have trained, validated, and benchmarked RNA-sequencing based gene expression SSP models for conventional clinical markers, molecular subtypes, and ROR in the largest, consecutive, primary BC cohort reported worldwide to date. Importantly, the observational population-based SCAN-B cohort is representative of contemporary stage-distribution and treatments, with sampling of fresh tumor tissue completely integrated in parallel with clinical routines [20,22] and with a complete turn-around assay time compliant with clinical usage (see Supplemental methods). These characteristics strongly support that results based on this cohort can be extended and generalized to the national BC population in Sweden, and other populations with comparable demographics.

The SSP classifications for conventional markers were validated against clinical pathology data from NKBC and against consensus status from independent re-assessment by three pathologists in the ABiM cohort [24] (Figure 1c). The concordance was high for ER, PR and HER2. For ER and PR results are well in line with previous studies confirming that sequencing-based assays can accurately mimic readouts from current commercial assays [24,47,48]. However, for any marker that is a direct target for treatment, such as the ER and HER2 receptors, special considerations regarding practical use of surrogate assays are required. For example, for HER2, the negative predictive value was very high for all SSP models (NPV=0.98). Considering that the Swedish *HER2* amplification rate in 2019 was 13.5% [25] this would imply that the sequencing-based classifiers could drastically reduce the number of negative tests performed. The lower positive predictive value of HER2 could be explained by differences in assessments. While histochemical or *in situ* hybridization scoring takes only stained invasive cancer cells into account, gene expression is measured from bulk RNA extracts including intraductal components. Moreover, the SSP models may also capture elevated HER2 signals present in tumors without HER2 protein overexpression or gene amplification. This suggests that a positive SSP HER2 scoring should be complemented with *in situ* (FFPE HER2 IHC/ISH) measurements to assure a correct status for anti-HER2 treatment decisions. On the other hand, tumors with elevated HER2 signal but without protein overexpression or gene amplification may potentially be sensitive to other treatments targeting the HER2 signaling pathway, which should be further addressed. In contrast to ER, PR and HER2, the SSP classifications for the proliferation marker Ki67 and NHG had lower accuracy. This may be expected as these conventional markers are routinely assessed by means that have been reported as sensitive to subjective and inter-observer variability [24,49-51]. Perhaps more importantly, the sequencing-based predictor showed very high negative predictive values for NHG Grade 1 and 3 tumors, while for the more heterogeneous NHG Grade 2 tumors the sequencing-based classification showed the ability to stratify patients into subsets with different clinical outcome, representing actual clinical value, in line with previous studies in the field [24,43,44].

A primary focus of this study was to derive SSP models for molecular subtypes and ROR scores in BC that would closely mimic conventional nearest centroid classifications, while being more applicable for inclusion in routine diagnostics of early BC. To achieve this, we used a meticulous normalization approach to generate suitable centroid training labels, followed by conventional class agreement analysis, patient outcome analysis, benchmarking versus Prosigna, and assessment of the impact on treatment recommendation (Figure 1b). Consistently, concordance evaluated in the independent test was high to very high (85-90%) between SSP subtype models (SSP-PAM50 and SSP-Subtype) and corresponding NCN classifications. Moreover, the main classification discrepancies were observed at the expected boundaries between the Luminal A and Luminal B subtypes, and between the Luminal A and Normal-like subtypes. This is not surprising given the underlying definition for discriminating between the subtypes, for which the distinction between Luminal A and B is determined by the ratio of relative correlations to the respective centroids. In reality there is no distinct separation in the underlying data discriminating between these two subtypes, rather, they are two ends of the same spectrum of relative ratios. Thus, cases in the middle of the spectrum are no more Luminal A than Luminal B or vice versa, similar to the seamless transition between varying degrees of some biological processes such as cell proliferation [52,53]. The same reasoning applies with more clarity to the ROR risk classification where original cut-points in ROR score between classes are set to achieve chosen incidences of disease recurrence. Although the coefficients for ROR score are derived to model risk of recurrence, it is still an association to risk of recurrence, i.e. a clinical endpoint. As such, there are no distinct underlying transitions between degrees of ROR score. Nonetheless, high agreement between SSP

and NCN classifications were observed for ROR risk classifications as well as for a two-group comparison combining ROR Low and Intermediate risk classification into one category (Supplemental Table 2). Importantly, the high agreement was also mirrored on a group level by similar prognostic performance for SSP and NCN models when assessed in the independent test data (Figure 2), particularly within the relevant clinical subgroup of post-menopausal (>50 years) ER+/HER2-/N0 BC treated with endocrine treatment alone (Figures 2c-g). Although the clinical event definition in our analysis (BCFi) differs from that used in validation of the Prosigna test (distant recurrence), these analyses suggest that SSP and NCN models are exchangeable on a group level concerning prognostic value. Moreover, our results demonstrate that SSP models are on their own capable of further stratifying current clinical subgroups of BC into subgroups with different clinical outcome, representing potential real clinical value.

An important aspect of the current study compared to existing academic studies in the field is the benchmarking of SSP classifications to actual matched clinical Prosigna classification, or Prosigna classification based on non-clinical Nanostring data, in two external clinical cohorts. Despite the external series being comparatively small, the comparisons provide important insight and benchmarking against results from an available and validated assay that is in clinical use today. These direct class comparisons demonstrated moderate to high numerical agreements and broadly high numerical agreements in pooled analysis. When interpreting the benchmarking results, tissue heterogeneity and sampling procedure need to be acknowledged as potential sources of discordance. This was also highlighted by Nielsen et al. for the clinical Prosigna assay, reporting 90% and 93% average agreement of ROR risk category for N0 and N+ patients, respectively, based on analysis at different laboratory sites using different tissue sections from the same tissue blocks [42]. Whereas Prosigna prescribes input material from FFPE sections verified to comprise a minimum of 10% invasive component, the RNA-sequencing based SSPs uses input material from fresh macro-dissected tumor tissue. This prevents strict direct comparisons of models even when samples originate from the same tumor. To investigate this issue, we also compared results from the SSP and Prosigna models with measurements from identically sourced RNA aliquots from fresh macro-dissected tissue. Notably, this improved the classification agreement for Subtype, decreased agreement for ROR risk category, while agreement for binary ROR risk classification remained the same. Importantly, performance for Prosigna from macroscopically evaluated fresh tissue against Prosigna from FFPE was in line with the corresponding agreements between SSP and Prosigna on FFPE. There are some weaknesses in these comparisons such as small sample size and diverging from Prosigna prescribed protocols; nonetheless, they highlight the soft transitions between classes and that exact agreement is neither expected nor needed for equivalence in practice as suggested by Bartlett et al.[5].

Although the SSP versus Prosigna classification agreement was not perfect, the concordance was high compared to reported agreement levels for different multigene assays [21,54,55], extending to clinical tests individually approved for the same use [5]. Notably, in those studies different multigene assays showed far from perfect agreement on an individual sample basis. In contrast, up to 89% direct agreement between SSP and Prosigna as observed for binary ROR risk category in this study infers not only similar group level characteristics, but also high agreement to Prosigna results on the sample level, although continued confirmation is needed as larger cohorts with data for both assays becomes available.

Concluding that SSP classifications are at the least comparable to Prosigna classification on a population level, we next examined the naïve impact on treatment decisions had SSP results been available to guide recommendation of adjuvant chemotherapy. Acknowledging that guidelines have changed during the years of patient recruitment, the estimations presented here remain somewhat uncertain. Moreover, in clinical practice the molecular classification would only be one part of the decision process as multidisciplinary teams, when recommending treatment, also consider co-morbidity and patient preferences. Such factors have not been accounted for in our analysis even though we restricted the assessment groups to age 51-70 years to reduce the effect of old age and accompanying co-morbidity. Moreover, we compared emulated treatment considerations with registry data for administered treatment, thus our estimates remain to be confirmed by future prospective evaluation. Nonetheless, our assessments suggest that naïve usage of SSP recommendations for treatment decisions would lead to a modest net change in use of adjuvant chemotherapy for ER+/HER2-/N0 BC in Sweden. This contrasts an observation in a North American population of early-stage BC, where a 70-gene signature identified a significant proportion of clinically high-risk patients that might not require chemotherapy [2]. However, hitherto presented data on change of therapy for the Prosigna test is more in line with our results [56]. Still, our results highlight that within ER+/HER2-/N0 early-stage disease diagnosed at >50≤70 years as much as 17% of cases may be subjects for changed chemotherapy recommendations as a result of molecular subtyping. In this study we did not include the corresponding assessment in node positive disease, as current national guidelines do not include these. However, it seems likely that a similar or even larger fraction of cases in this group would be subjects for changed treatment recommendations as a

result of molecular subtyping.

The clinical usefulness of currently available and validated multigene assays is limited to certain subgroups of BC patients. For instance, in Sweden the recently added recommendation in the national guidelines [25] to use molecular diagnostics was limited to early-stage postmenopausal ER+/HER2-/N0 BC. Moreover, current clinical gene expression-based assays are associated with a substantial financial cost, may require sending samples outside a regional healthcare region, and typically report a single assay output, e.g., a treatment recommendation for a specific patient population. Considering that modern cancer diagnostics require a multitude of molecular diagnostic procedures, generic analysis that can provide several clinically relevant readouts will likely become even more important in the near future. In this context, a broad sequencing-based assay, like RNA-sequencing, to generate generic transcriptome data, from which a multitude of different readouts can be derived, presents an attractive alternative. In addition to the current study suggesting that RNA-sequencing can provide benchmarked intrinsic subtype and ROR scores, RNA-sequencing has also been reported to be able to provide reliable models for current conventional BC biomarkers [24,47,48] and to identify expressed somatic mutations in for example *ESR1* and *PIK3CA* [57,58] that may be important for future clinical management. Moreover, an upfront testing of breast cancer cases irrespective of subtype would cut lead-times for molecular assay results and may also allow future implementation of prognostic/treatment predictive signatures for clinical subgroups, like TNBC and *HER2*-amplified cases, for which there are none in clinical use today.

In summary, we demonstrate the potential of RNA-sequencing as a multipurpose assay for diagnostics and treatment decision support in early breast cancer. Based on a single analysis of fresh tissue procured at the time of diagnosis at regional pathology departments without special sampling requirements we demonstrate the potential to derive benchmarked equivalent estimates of current clinical markers and molecular subtypes and risk assessments, which may be extended to include mutational calls for key driver genes. Importantly, a completely open assay coupled with regionally performed sequencing, as part of routine healthcare after required validation and quality assurance, may be of strong clinical and socioeconomic value. This is demonstrated by the potential to reduce current single diagnostic marker analyses, but also the clear evidence that the gene expression-based stratification can separate otherwise seemingly homogenous clinical subgroups of breast cancer into groups with clinically relevant diverse outcomes.

Acknowledgements

The authors would like to acknowledge patients, clinicians, and hospital staff participating in the SCAN-B study, the staff at the central SCAN-B laboratory at Division of Oncology, Lund University, the Swedish National Quality Register for Breast Cancer (NKBC), Regional Cancer Center South, and the South Swedish Breast Cancer Group (SSBCG). Oslo Breast Cancer Research Consortium (OSBREAC).

Funding

Financial support for this study was provided by the Swedish Cancer Society (CAN 2016/659, CAN 2018/685, CAN 2021/1407 and a 2018 Senior Investigator Award [JS: SIA190013]), the Mrs Berta Kamprad Foundation (FBKS 2018-3, FBKS-2020-5 and FBKS-2020-9), the Lund-Lausanne L2-Bridge/Biltema Foundation (F 2016/1330), the Mats Paulsson Foundation (IACD 2017), and Swedish governmental funding (ALF, grant 2018/40612). Work on the ABiM cohort was supported by Bröstcancerförbundet. The OSLO2-EMIT0 was funded by grants from The Norwegian Cancer Society (420056), South-Eastern Norway Regional Health Authority (2012071) and open access funding provided by Oslo University Hospital.

Competing interests

The authors declare that they have no competing interests. AE has received speakers' honoraria from Novartis, Amgen, Roche, and advisory board fees from Roche. HL reports honoraria for lecturing from Astra-Zeneca, Novartis, Lilly, and Seagen, and working in advisory boards of Pfizer, Novartis, Daiichi, MSD, Amgen, and Pierre Fabre, and has received research support from Roche. LHS has employment and ownership interest (including stock and patents) in SAGA Diagnostics AB.

References

1. Goldhirsch, A., *et al.* Personalizing the treatment of women with early breast cancer: highlights of the St Gallen International Expert Consensus on the Primary Therapy of Early Breast Cancer 2013. *Ann Oncol* **24**, 2206-2223 (2013).
2. Cardoso, F., *et al.* 70-Gene Signature as an Aid to Treatment Decisions in Early-Stage Breast Cancer. *The New England journal of medicine* **375**, 717-729 (2016).
3. Gnant, M., *et al.* Predicting distant recurrence in receptor-positive breast cancer patients with limited clinicopathological risk: using the PAM50 Risk of Recurrence score in 1478 postmenopausal patients of the ABCSG-8 trial treated with adjuvant endocrine therapy alone. *Ann Oncol* **25**, 339-345 (2014).
4. Sparano, J.A., *et al.* Adjuvant Chemotherapy Guided by a 21-Gene Expression Assay in Breast Cancer. *The New England journal of medicine* **379**, 111-121 (2018).
5. Bartlett, J.M., *et al.* Comparing Breast Cancer Multiparameter

Tests in the OPTIMA Prelim Trial: No Test Is More Equal Than the Others. *Journal of the National Cancer Institute* **108**(2016).
6. Andre, F., *et al.* Use of Biomarkers to Guide Decisions on Adjuvant Systemic Therapy for Women With Early-Stage Invasive Breast Cancer: ASCO Clinical Practice Guideline Update-Integration of Results From TAILORx. *J Clin Oncol* **37**, 1956-1964 (2019).
7. Parker, J.S., *et al.* Supervised risk predictor of breast cancer based on intrinsic subtypes. *J Clin Oncol* **27**, 1160-1167 (2009).
8. Wallden, B., *et al.* Development and verification of the PAM50-based Prosigna breast cancer gene signature assay. *BMC Med Genomics* **8**, 54 (2015).
9. Laenkholm, A.V., *et al.* Population-based Study of Prosigna-PAM50 and Outcome Among Postmenopausal Women With Estrogen Receptor-positive and HER2-negative Operable Invasive Lobular or Ductal Breast Cancer. *Clinical breast cancer* **20**, e423-e432 (2020).
10. Laenkholm, A.V., *et al.* PAM50 Risk of Recurrence Score Predicts 10-Year Distant Recurrence in a Comprehensive Danish Cohort of Postmenopausal Women Allocated to 5 Years of Endocrine Therapy for Hormone Receptor-Positive Early Breast Cancer. *J Clin Oncol* **36**, 735-740 (2018).
11. Gnant, M., *et al.* Identifying clinically relevant prognostic subgroups of postmenopausal women with node-positive hormone receptor-positive early-stage breast cancer treated with endocrine therapy: a combined analysis of ABCSG-8 and ATAC using the PAM50 risk of recurrence score and intrinsic subtype. *Ann Oncol* **26**, 1685-1691 (2015).
12. Ohnstad, H.O., *et al.* Prognostic value of PAM50 and risk of recurrence score in patients with early-stage breast cancer with long-term follow-up. *Breast Cancer Res* **19**, 120 (2017).
13. Picornell, A.C., *et al.* Breast cancer PAM50 signature: correlation and concordance between RNA-Seq and digital multiplexed gene expression technologies in a triple negative breast cancer series. *BMC Genomics* **20**, 452 (2019).
14. Paquet, E.R. & Hallett, M.T. Absolute assignment of breast cancer intrinsic molecular subtype. *Journal of the National Cancer Institute* **107**, 357 (2015).
15. Sorlie, T., *et al.* The importance of gene-centring microarray data. *The lancet oncology* **11**, 719-720; author reply 720-711 (2010).
16. Staaf, J. & Ringner, M. Making breast cancer molecular subtypes robust? *Journal of the National Cancer Institute* **107**, 386 (2015).
17. Ringner, M., Jonsson, G. & Staaf, J. Prognostic and Chemotherapy Predictive Value of Gene-Expression Phenotypes in Primary Lung Adenocarcinoma. *Clin Cancer Res* **22**, 218-229 (2016).
18. Afsari, B., Fertig, E.J., Geman, D. & Marchionni, L. switchBox: an R package for k-Top Scoring Pairs classifier development. *Bioinformatics* **31**, 273-274 (2015).
19. Cirenajwis, H., Lauss, M., Planck, M., Vallon-Christersson, J. & Staaf, J. Performance of gene expression-based single sample predictors for assessment of clinicopathological subgroups and molecular subtypes in cancers: a case comparison study in non-small cell lung cancer. *Briefings in bioinformatics* **21**, 729-740 (2020).
20. Saal, L.H., *et al.* The Sweden Cancerome Analysis Network - Breast (SCAN-B) Initiative: a large-scale multicenter infrastructure towards implementation of breast cancer genomic analyses in the clinical routine. *Genome Med* **7**, 20 (2015).
21. Vallon-Christersson, J., *et al.* Cross comparison and prognostic assessment of breast cancer multigene signatures in a large population-based contemporary clinical series. *Sci Rep* **9**, 12184 (2019).
22. Ryden, L., *et al.* Minimizing inequality in access to precision medicine in breast cancer by real-time population-based molecular analysis in the SCAN-B initiative. *Br J Surg* **105**, e158-e168 (2018).
23. Shamseddin, M., *et al.* Contraceptive progestins with androgenic properties stimulate breast epithelial cell proliferation. *EMBO Mol Med*, e14314 (2021).
24. Brueffer, C., *et al.* Clinical Value of RNA Sequencing-Based Classifiers for Prediction of the Five Conventional Breast Cancer Biomarkers: A Report From the Population-Based Multicenter Sweden Cancerome Analysis Network-Breast Initiative. *JCO Precis Oncol* **2**(2018).
25. National Quality Registry for breast cancer - Sweden. https://cancercentrum.se/samverkan/cancerdiagnoser/brost/kvalitetsregister/. Accessed: 2021. Nov 12
26. Swedish Society of Pathology. www.svfp.se/kvastdokument. Accessed: 2021. Nov 26
27. Staaf, J., *et al.* Whole-genome sequencing of triple-negative breast cancers in a population-based clinical study. *Nature medicine* **25**, 1526-1533 (2019).
28. Aure, M.R., *et al.* Integrative clustering reveals a novel split in the luminal A subtype of breast cancer with impact on outcome. *Breast Cancer Res* **19**, 44 (2017).
29. Winter, C., *et al.* Targeted sequencing of BRCA1 and BRCA2 across a large unselected breast cancer cohort suggests that one-third of mutations are somatic. *Ann Oncol* **27**, 1532-1538 (2016).
30. Tekpli, X., *et al.* An independent poor-prognosis subtype of breast cancer defined by a distinct tumor immune microenvironment. *Nat Commun* **10**, 5499 (2019).
31. Picard tools. https://broadinstitute.github.io/picard/. Accessed: 2021. Nov 12
32. Bolger, A.M., Lohse, M. & Usadel, B. Trimmomatic: a flexible trimmer for Illumina sequence data. *Bioinformatics* **30**, 2114-2120 (2014).
33. Langmead, B. & Salzberg, S.L. Fast gapped-read alignment with Bowtie 2. *Nature methods* **9**, 357-359 (2012).
34. Kim, D., Langmead, B. & Salzberg, S.L. HISAT: a fast spliced aligner with low memory requirements. *Nature methods* **12**, 357-360 (2015).
35. Kim, D., Paggi, J.M., Park, C., Bennett, C. & Salzberg, S.L. Graph-based genome alignment and genotyping with HISAT2 and HISAT-genotype. *Nature biotechnology* **37**, 907-915 (2019).
36. Pertea, M., *et al.* StringTie enables improved reconstruction of a transcriptome from RNA-seq reads. *Nature biotechnology* **33**, 290-295 (2015).
37. dbSNP. https://www.ncbi.nlm.nih.gov/SNP/. Accessed: 2021. Nov 12
38. Frankish, A., *et al.* GENCODE reference annotation for the human and mouse genomes. *Nucleic acids research* **47**, D766-D773 (2019).
39. AIMS GitHub repository. https://github.com/meoyo/trainAIMS. Accessed: 2021. Nov 12
40. Gourgou-Bourgade, S., *et al.* Guidelines for time-to-event end point definitions in breast cancer trials: results of the DATECAN initiative (Definition for the Assessment of Time-to-event Endpoints in CANcer trials)dagger. *Ann Oncol* **26**, 873-879 (2015).
41. Brooke, H.L., *et al.* The Swedish cause of death register. *Eur J Epidemiol* **32**, 765-773 (2017).
42. Nielsen, T., *et al.* Analytical validation of the PAM50-based Prosigna Breast Cancer Prognostic Gene Signature Assay and nCounter Analysis System using formalin-fixed paraffin-embedded breast tumor specimens. *BMC cancer* **14**, 177 (2014).
43. Sotiriou, C., *et al.* Gene expression profiling in breast cancer: understanding the molecular basis of histologic grade to improve prognosis. *Journal of the National Cancer Institute* **98**, 262-272 (2006).
44. Ivshina, A.V., *et al.* Genetic reclassification of histologic grade delineates new clinical subtypes of breast cancer.

Cancer research **66**, 10292-10301 (2006).
45. Lofgren, L.*, et al.* Validation of data quality in the Swedish National Register for Breast Cancer. *BMC Public Health* **19**, 495 (2019).
46. Sorlie, T.*, et al.* Repeated observation of breast tumor subtypes in independent gene expression data sets. *Proceedings of the National Academy of Sciences of the United States of America* **100**, 8418-8423 (2003).
47. Rantalainen, M.*, et al.* Sequencing-based breast cancer diagnostics as an alternative to routine biomarkers. *Sci Rep* **6**, 38037 (2016).
48. Bastani, M.*, et al.* A machine learned classifier that uses gene expression data to accurately predict estrogen receptor status. *PLoS ONE* **8**, e82144 (2013).
49. Stalhammar, G.*, et al.* Digital image analysis of Ki67 in hot spots is superior to both manual Ki67 and mitotic counts in breast cancer. *Histopathology* **72**, 974-989 (2018).
50. Acs, B.*, et al.* Variability in Breast Cancer Biomarker Assessment and the Effect on Oncological Treatment Decisions: A Nationwide 5-Year Population-Based Study. *Cancers (Basel)* **13**(2021).
51. Nielsen, T.O.*, et al.* Assessment of Ki67 in Breast Cancer: Updated Recommendations From the International Ki67 in Breast Cancer Working Group. *Journal of the National Cancer Institute* **113**, 808-819 (2021).
52. Desmedt, C.*, et al.* Biological processes associated with breast cancer clinical outcome depend on the molecular subtypes. *Clin Cancer Res* **14**, 5158-5165 (2008).
53. Mackay, A.*, et al.* Microarray-based class discovery for molecular classification of breast cancer: analysis of interobserver agreement. *Journal of the National Cancer Institute* **103**, 662-673 (2011).
54. Fan, C.*, et al.* Concordance among gene-expression-based predictors for breast cancer. *The New England journal of medicine* **355**, 560-569 (2006).
55. Buus, R.*, et al.* Molecular Drivers of Oncotype DX, Prosigna, EndoPredict, and the Breast Cancer Index: A TransATAC Study. *J Clin Oncol* **39**, 126-135 (2021).
56. Ontario, H. Gene Expression Profiling Tests for Early-Stage Invasive Breast Cancer: A Health Technology Assessment. *Ont Health Technol Assess Ser* **20**, 1-234 (2020).
57. Brueffer, C.*, et al.* The mutational landscape of the SCAN-B real-world primary breast cancer transcriptome. *EMBO Mol Med*, e12118 (2020).
58. Dahlgren, M.*, et al.* Preexisting Somatic Mutations of Estrogen Receptor Alpha (ESR1) in Early-Stage Primary Breast Cancer. *JNCI Cancer Spectr* **5**, pkab028 (2021).

Supplemental Tables 1-6

Supplemental Table 1. Selected SSP gene-rules for SSP-PAM50 (five groups) model, SSP-Subtype (four groups) model and SSP-ROR model.

SSP-PAM50 (5 groups)		SSP-Subtype (4 groups)		SSP-ROR					
Gene rules	Class	Gene rules	Class	Gene rules	Class	cont.	cont.	cont.	cont.
IGF1R<GRB7	Her2	IGF1R<GRB7	Her2	TOP2A<ZNF507	c005	MYBL2<BOC	c035	FAM122A<CCNA2	c065
RERG<CDK12	Her2	RERG<CDK12	Her2	RRM2<MID1	c005	EXO1<CACH1	c035	TMEM237<MELK	c065
DBNDD2<STARD3	Her2	DBNDD2<STARD3	Her2	UBE2C<TSHZ2	c005	TICRR<GREM2	c035	NEK1<CEP55	c065
SLC39A6<ERBB2	Her2	SLC39A6<ERBB2	Her2	NCAPH<KLHL29	c005	UBE2C<LHFPL6	c035	TTC28<KIF4A	c065
RND2<TCAP	Her2	RND2<TCAP	Her2	BIRC5<CCDC28	c005	BIRC5<MYH11	c035	MAP2K5<CCNB2	c065
ESR1<PGAP3	Her2	ESR1<PGAP3	Her2	MKI67<EVC2	c005	MELK<SPRY2	c035	CDADC1<NCAPG	c065
BCL2<CCNB2	Her2	BCL2<CCNB2	Her2	CCNB2<SNCAIP	c005	BUB1<JAM2	c035	RFX7<BUB1B	c065
PPM1J<C2orf54	Her2	PPM1J<C2orf54	Her2	TPX2<ZNF438	c005	CENPA<C2orf40	c035	PCIF1<UBE2C	c065
CDON<MFSD2A	Her2	CDON<MFSD2A	Her2	KIF4A<EPHB1	c005	CLSPN<SCN4B	c035	ZBTB40<SPAG5	c065
CSAR2<FA2H	Her2	CSAR2<FA2H	Her2	KIF20A<GREM2	c005	CKAP2L<MAMDC2	c035	HMG20A<NUSAP1	c065
RBBP8<RRM2	Her2	TBC1D9<MIEN1	Her2	CCNA2<PDE7B	c005	CCNB2<LAMA2	c035	SNX33<KIFC1	c065
TBC1D9<MIEN1	Her2	RBBP8<RRM2	Her2	PTTG1<ITGA9	c005	CCNA2<MED28	c035	SPEN<PTTG1	c065
STC2<TRIB3	Her2	MAPT<MYBL2	Her2	HMMR<THSD7A	c005	MTFR2<FAT4	c035	WDR33<TPX2	c065
MAPT<MYBL2	Her2	STC2<TRIB3	Her2	DLGAP5<CEP85L	c005	AURKB<MGFR	c035	SIK2<MKI67	c065
IL6ST<ACTR3	Her2	THSD4<CDC20	Her2	NUSAP1<SHE	c005	NCAPH<RHOJ	c035	FBXO42<AURKA	c065
THSD4<CDC20	Her2	IL6ST<ACTR3	Her2	PLK1<PRX	c005	TPX2<ZCCHC24	c035	MINT<PLK1	c065
BUB1<ALMS1	LumA	CCDC170<HIURP	Her2	CKAP2L<NLGN3	c005	MKI67<SLIT2	c035	PTPN21<BUB1	c065
C1orf226<FGFR4	Her2	PCSK6<TMEM86A	Her2	MELK<PRDM5	c005	CEP55<PCDH18	c035	PRMT9<NDC80	c065
PCSK6<TMEM86A	Her2	C1orf226<FGFR4	Her2	AURKA<GPRASP1	c005	HIURP<PAMR1	c035	TRIM65<BIRC5	c065
PARD6B<CENPA	Her2	PARD6B<CENPA	Her2	CDK1<TRIM23	c005	BUB1B<ARHGAP19	c035	RHOJ<KIF20A	c065
TPRG1<SHCBP1	Her2	TPRG1<SHCBP1	Her2	DEPDC1<ZNF891	c005	CDCA5<LMOD1	c035	ZNF429<KIF11	c065
PCM1<GSR	Her2	BUB1<ARHGAP19	LumA	UBE2C<RASL12	c010	SGO1<MAMDC2	c040	MED28<CCNA2	c070
LONRF2<TICRR	Her2	CEP55<MED28	LumA	NUSAP1<FAM122A	c010	TPX2<SH3D19	c040	MAP2K5<CCNB2	c070
NEK10<FUT3	Her2	NCAPG<LCA5	LumA	CEP55<GPRASP1	c010	MYBL2<MYH11	c040	ZNF777<MYBL2	c070
BUB1<ALMS1	LumA	TICRR<TRABD2B	LumA	RRM2<TSHZ2	c010	CEP55<SPRY2	c040	AASS<CKAP2L	c070
CEP55<MED28	LumA	CCNB2<MAP2K5	LumA	TPX2<ST3GAL3	c010	CKAP2L<SCN4B	c040	ZNF691<KIF2C	c070
NCAPG<LCA5	LumA	CCNA2<FAM122A	LumA	CCNA2<C8orf88	c010	CENPA<CLDN11	c040	ASXL1<TPX2	c070
AURKB<PFAS	LumA	AURKB<PFAS	LumA	BUB1<DNAJC18	c010	BUB1<SLIT2	c040	ZER1<UBE2C	c070
CCNB2<MAP2K5	LumA	MYBL2<BOC	LumA	TOP2A<ITGA9	c010	TICRR<TRABD2B	c040	HERC2<MKI67	c070
CCNA2<NEK1	LumA	UBE2C<NCOA5	LumA	DLGAP5<PDE7B	c010	MCM10<TSHZ2	c040	PFAS<AURKB	c070
MYBL2<PPP1R26	LumA	MCM10<GPRASP1	LumA	MELK<PREX2	c010	NCAPH<CEP68	c040	RFXAP<SGO1	c070
RRM2<DIXDC1	LumA	RRM2<DIXDC1	LumA	NDC80<ADPRM	c010	ARHGAP19<BUB1	c040	ARHGAP19<BUB1	c070
UBE2C<NCOA5	LumA	HIURP<SCN4B	LumA	ANLN<MOB3B	c010	NUF2<ARHGAP19	c040	CTC1<SPAG5	c070
NDC80<ZSCAN30	LumA	NDC80<PRMT9	LumA	ASPM<PDE1C	c010	MELK<LAMA2	c040	PMS1<CEP55	c070
TPX2<CHD6	LumA	TPX2<CHD6	LumA	KIF4A<KLHL29	c010	UBE2C<FBLN5	c040	FAM122A<MELK	c070
KIF4A<UBXN10	LumA	FAM83D<TTC28	LumA	BIRC5<PRDM11	c010	EXO1<PPP1R12B	c040	MMNAT1<KIF4A	c070
SPAG5<STK36	LumA	PLK1<SETD1A	LumA	HIURP<PCHHP	c010	SHCBP1<CACHD1	c040	ZBTB40<CDCA8	c070
TICRR<TRABD2B	LumA	MELK<RHOJ	LumA	MKI67<PLEKHM3	c010	RACGAP1<DOCK1	c040	DNAJC27<DEPDC1B	c070
PLK1<SETD1A	LumA	MKI67<HERC2	LumA	MYBL2<TESC	c010	KIF20A<LMOD1	c040	WDFY2<CENPA	c070
MKI67<ZBTB40	LumA	PTTG1<CWC27	LumA	NEIL3<TSLP	c010	FAM83D<SIK2	c040	TMEM39B<PLK1	c070
PTTG1<CWC27	LumA	KIF11<IKZF5	LumA	KIF14<PAK3	c010	PLK1<CDK7	c040	CBX7<BIRC5	c070
NUSAP1<MYO5C	LumA	BIRC5<SNX33	LumA	KIF23<ZNF333	c010	BIRC5<TINAGL1	c040	BORCS7<CDK1	c070
HIURP<ZBTB3	LumA	TRIM29<IQGAP3	LumB	CCNB2<SCN4B	c015	RRM2<ZNF106	c045	MRPS14<UBE2T	c075
BIRC5<SNX33	LumA	SFRP1<NEK2	LumB	BUB1<MOB3B	c015	TPX2<SH3D19	c045	CCDC115<UBE2C	c075
KIF11<IKZF5	LumA	KRT5<TPX2	LumB	NDC80<GPRASP1	c015	PRR11<RHOJ	c045	CREBRF<BUB1	c075
MCM10<C4orf36	LumA	MIA<ESPL1	LumB	HIURP<KLHL29	c015	MCM10<SCN4B	c045	TFCP2<TPX2	c075
CDCA5<SLC35E2	LumA	KRT17<UBE2C	LumB	UBE2C<BOC	c015	FAM83D<ARHGEF10	c045	ZYG11B<CEP55	c075
SGO1<CFAP69	LumA	EGFR<HMMR	LumB	MKI67<TSHZ2	c015	CDCA5<SNX33	c045	HERC2<CDCA5	c075
TRIM29<IQGAP3	LumB	KRT16<SPC24	LumB	NUSAP1<RHOJ	c015	SGO1<MSANTD2	c045	TYW3<AURKA	c075
SFRP1<NEK2	LumB	FOXC1<SGO1	LumB	BIRC5<ASB1	c015	BUB1<PARP16	c045	SETD1A<PLK1	c075
KRT5<TPX2	LumB	KLK5<NEIL3	LumB	BUB1B<PLEKHM3	c015	UBE2C<RBFOX2	c045	CEP68<CCNA2	c075
MIA<ESPL1	LumB	KRT8/18<CDC25C	LumB	RRM2<ERG	c015	KIFC1<CBX7	c045	MED28<MELK	c075
KRT17<UBE2C	LumB	STAC2<E2F8	LumB	NEK2<CACHD1	c015	TICRR<KLHL3	c045	INTS5<MYBL2	c075
EGFR<HMMR	LumB	KLK6<TICRR	LumB	CEP55<PLA2R1	c015	ANLN<PDGFD	c045	LAMA2<KIF20A	c075
KRT16<SPC24	LumB	DSC3<KIF14	LumB	KIF4A<ARHGAP19	c045	KIF4A<ARHGAP19	c045	CALCOCO1<PTTG1	c075
FOXC1<SGO1	LumB	PPP1R14C<POLQ	LumB	TPX2<FBXO42	c015	PLK1<CAMTA2	c045	METTL16<SPAG5	c075
KLK5<NEIL3	LumB	FAM171A1<KIF4A	LumB	TOP2A<SPRY2	c015	NEK2<LZTFL1	c045	PFAS<AURKB	c075
KRT6B<CDC25C	LumB	SERPINB5<CKAP2L	LumB	MELK<C8orf88	c015	RACGAP1<COL4A3BP	c045	ZC3H6<SGO1	c075
STAC2<E2F8	LumB	CRYAB<PTTG1	LumB	PLK1<S1PR2	c015	MELK<CDC37L1	c045	ZBTB40<CDCA8	c075
KLK6<TICRR	LumB	SOX10<RIF1BB	LumB	KIF18B<PHYHIP	c015	MKI67<CEP68	c045	TN52<TACC3	c075
DSC3<KIF14	LumB	ID4<DTL	LumB	ASPM<SAMD5	c015	NUF2<TRIM23	c045	NCDA1<RRM2	c075
PPP1R14C<POLQ	LumB	GABRP<SPC25	LumB	MYBL2<OSR1	c015	HIURP<TTC28	c045	TRABD2B<TICRR	c075
FAM171A1<KIF4A	LumB	KRT14<UBE2T	LumB	CCNA2<MAMDC2	c015	EXO1<NAPEPLD	c045	ARHGAP19<NDC80	c075
SERPINB5<CKAP2L	LumB	FOXA1<ATP2C1	Basal	KIF20A<TSHZ2	c020	BOC<UBE2C	c050	MTMR10<CEP55	c080
SOX10<KIF18B	LumB	MLPH<SLC43A3	Basal	CEP55<CACHD1	c020	TSHZ2<BUB1	c050	CEP68<BUB1	c080
CRYAB<PTTG1	LumB	PRR15<FOXC1	Basal	BIRC5<TTC28	c020	CACHD1<NCAPH	c050	EZH1<SPAG5	c080
ID4<DTL	LumB	TTC6<BCL11A	Basal	MELK<LCA5	c020	STAC<KIF14	c050	GID4<PRR11	c080
GABRP<SPC25	LumB	AGR2<RARRES1	Basal	MKI67<CLDN11	c020	SMAD9<ORC6	c050	ZBTB20<HIURP	c080
KRT14<UBE2T	LumB	TBC1D9<RBMS1	Basal	TPX2<CEP68	c020	CLDN11<CCNB2	c050	ACTR8<AURKA	c080
BOC<ASF1B	LumB	ZMYND10<TMCC2	Basal	KIF2C<SCN4B	c020	CYYR1<RRM2	c050	TNS2<MYBL2	c080
DSG3<E2F7	LumB	ATP8B1<DSC2	Basal	UBE2C<CBX7	c020	CEP55<SOCS5	c050	CCNDBP1<RRM2	c080
SYNM<PBK	LumB	AGR3<GABRP	Basal	DEPDC1<SAMD5	c020	SAMD5<SKA1	c050	POFUT1<TPX2	c080
MLPH<SLC43A3	Basal	THSD4<MAML2	Basal	MYBL2<IL34	c020	SLIT2<TPX2	c050	PKIG<UBE2C	c080
FOXA1<PLSCR1	Basal	SPDEF<TSC22D4	Basal	CCNB2<EGFR	c020	SCN3B<POLQ	c050	ATG14<DLGAP5	c080
PRR15<FOXC1	Basal	CER56<ANP32E	Basal	RRM2<SPRY2	c020	PSAT1<EBCCGL	c050	SLU7<PTTG1	c080
TTC6<TBX19	Basal	SLC44A4<KLF5	Basal	HIURP<GPRASP1	c020	C8orf88<EXO1	c050	DCAKD<BIRC5	c080
AGR2<RARRES1	Basal	ANXA9<CDCA7	Basal	BUB1<MAMDC2	c020	OSR1<MYBL2	c050	ZNF592<CDCA5	c080
ATP8B1<DSC2	Basal	ZNF552<SFT2D2	Basal	EXO1<GNAL	c020	ALX4<MCM10	c050	CAMTA2<PLK1	c080
TSPAN1<PSAT1	Basal	C9orf152<PSAT1	Basal	CDK1<SOCS5	c020	FOXC1<NDC80	c050	TMM22<AURKB	c080
TBC1D9<UBE2J1	Basal	ESR1<FAM171A1	Basal	KIF4A<WDFY2	c020	TMOD1<HIURP	c050	LRIG2<CKAP2L	c080
BCAS1<BCL11A	Basal	GATA3<RANBP1	Basal	MCM10<LRP4	c020	MOB3B<SPC25	c050	NAF1<CCNA2	c080
AGR3<GPM6B	Basal	XBP1<YBX1	Basal	NCAPH<ITGA9	c020	SCN4B<KIF20A	c050	WDR19<KIF4A	c080
ZMYND10<TMCC2	Basal	CAPN8<PPP1R14C	Basal	KIF11<RFX7	c020	RGMA<PLK1	c050	ARNT<UBE2T	c080
SLC44A4<KLF5	Basal	DNAH5<CHODL	Basal	FOXM1<MAPKBP1	c020	MATN2<PTTG1	c050	CDC37L1<MELK	c080
ANXA9<CDCA7	Basal			MELK<CACHD1	c025	SCN4B<KIF4A	c055	SIK3<SPAG5	c085
SPDEF<TSC22D4	Basal			PLK1<NGFR	c025	C8orf88<HIURP	c055	TOPORS<MELK	c085
TFF3<KCNN4	Basal			CCNB2<SPRY2	c025	BOC<CDC20	c055	ZWF3B0D<CEP55	c085
CER56<ANP32E	Basal			KIF4A<TSHZ2	c025	IL11RA<PLK1	c055	KDM3B<TPX2	c085
GATA3<MRPL9	Basal			CDC20<BOC	c025	LRCH1<TPX2	c055	BICRAL<CCNA2	c085
ZNF552<SFT2D2	Basal			CEP55<TMEM237	c025	NIPSNAP3B<MCM10	c055	ERCC6<KIF4A	c085
ESR1<NCAPH	Basal			MKI67<ITGA9	c025	SYN2<TICRR	c055	ZNF621<CENPA	c085
C9orf116<CCNE1	Basal			KIF15<GPRASP1	c025	ITGA9<MKI67	c055	TGFBRAP1<NCAPH	c085
CAPN8<PPP1R14C	Basal			BUB1<GPRASP2	c025	SLIT2<RRM2	c055	CCDC71<MYBL2	c085
THSD4<PTPN14	Basal			TPX2<AMOTL1	c025	EGFR<BUB1	c055	CRIM1<UBE2T	c085
DEGS2<KCNK5	Basal			CENPA<HLF	c025	JAM2<CCNB2	c055	ZC3H6<CKAP2L	c085
DNAH5<CHODL	Basal			UBE2C<MYH11	c025	SMAD9<DEPDC1B	c055	IL17RD<SGO1	c085
CGN<COL17A1	Normal			EXO1<SCN4B	c025	NGFR<MYBL2	c055	ZBTB20<MCM10	c085
MYB<MYH11	Normal			KIF14<SAMD5	c025	TF63<EXO1	c055	LRP6<FAM83D	c085
RSPH1<TSHZ2	Normal			POLQ<TMEM97B	c025	TCEAL7<NCAPG	c055	SKV15<CDCA5	c085
OPA1<PROS1	Normal			HIURP<HOXA5	c025	GPRASP1<SHCBP1	c055	TNKS<BUB1	c085
C2orf15<KLHL13	Normal			KIF1BB<TRABD2B	c025	PREX2<CENPE	c055	VAMP2<UBE2C	c085
CDG7<MATN2	Normal			MCM10<KLHL29	c025	MMRN2<UBE2C	c055	RBM22<PTTG1	c085
SPATA17<PDE1C	Normal			DLGAP5<DMD	c025	TSHZ2<KIF2C	c055	LCA5<MTFR2	c085
TESMIN<C2orf40	Normal			CCNA2<CLDN11	c025	FOXC1<CDC45	c055	MCC<CDC45	c085
OVOL2<NGFR	Normal			RRM2<LAMA2	c025	CEP68<PRC1	c055	SORBS1<ANLN	c085
CIPC<SPRY2	Normal			HIURP<SCN4B	c030	C20orf194<CEP55	c060	STX12<RRM2	c090
TRPS1<SFRP1	Normal			MCM10<GPRASP1	c030	GPRASP1<MCM10	c060	TMEM35B<CCNB2	c090
BLZF1<CFI	Normal			KIF4A<CLDN11	c030	LAMA2<TPX2	c060	MARCH8<NCAPH	c090
ESR1<KRT5	Normal			CENPA<MAMDC2	c030	ZCCHC24<UBE2C	c060	TMEM222<MYBL2	c090
MYO5B<SYNM	Normal			MYBL2<COL17A1	c030	SHE<HIURP	c060	TNS2<CDCA5	c090
MYO6<DST	Normal			BUB1<C20orf194	c030	SCN4B<CDC45	c060	SMAD4<CEP55	c090
CLUAP1<IL33	Normal			MELK<CACHD1	c030	MEIS2<KIF4A	c060	CRIM1<RACGAP1	c090
CCDC170<SCN4B	Normal			NCAPG<LCA5	c030	RNF180<CENPE	c060	MINDY1<BIRC5	c090
SMIM22<KRT14	Normal			UBE2C<MYH11	c030	CCDC86<MYBL2	c060	ZBTB20<CKAP2L	c090
ZMYND10<MIA	Normal			AURKB<RASL12	c030	SPRY2<CCNB2	c060	SIK3<BUB1	c090
GLYR1<PLPP3	Normal			PRR11<TSHZ2	c030	ARHGAP23<CDCA5	c060	CX3CR1<MTFR2	c090
B4GALNT4<OSR1	Normal			CEP55<RHOJ	c030	PGM5<BUB1	c060	UBIAD1<KIF2C	c090
SIAH2<CCL14	Normal			TPX2<POLR1E	c030	TCEANC2<CKAP2L	c060	YIPF4<CENPA	c090
CELSR1<TINAGL1	Normal			RRM2<PROS1	c030	MAPKBP1<SPAG5	c060	PLSCR4<MELK	c090
PLEKHA3<C8orf88	Normal			CCNB2<AMOTL1	c030	TCEAL7<SGO1	c060	POMGNT2<E2F1	c090
				CCNA2<IL17RD	c030	CACHD1<MELK	c060	KIF3B<TPX2	c090
				PLK1<BOC	c030	SIRT1<CDK1	c060	KLHL21<AURKB	c090
				SGO1<TP63	c030	FAM13C<CENPA	c060	CLCN6<SGO1	c090
				BIRC5<LMOD1	c030	ZBTB20<MKI67	c060	CBX7<TROAP	c090
				NDC80<PPP1R12B	c030	TTBK2<BUB1B	c060	ZNF76<KIFC1	c090
				EXO1<C2orf40	c030	FBXO34<TOP2A	c060	DOCK1<MKI67	c090

Supplemental Table 2. SSP prediction performance for subtypes and ROR categories validated against NCN classification in the independent population-based test set of early breast cancer.

		Accuracy			Kappa						
SSP model vs. NCN	**n**	**Accuracy**	**95% CI**	**AccuracyNull**	**Kappa**	**95% CI**	**class value**	**Sensitivity**	**Specificity**	**Pos Pred Value**	**Neg Pred Value**
PAM50	2357	0.85	(0.83, 0.86)	0.51	0.78	(0.76, 0.80)	Luminal A	0.83	0.96	0.96	0.85
							Luminal B	0.86	0.96	0.87	0.96
							Basal	0.87	1.00	0.97	0.99
							Her2-enriched	0.83	0.97	0.71	0.98
							Normal-like	0.90	0.93	0.41	0.99
Subtype	2343	0.90	(0.89, 0.91)	0.56	0.84	(0.82, 0.86)	Luminal A	0.92	0.96	0.96	0.91
							Luminal B	0.85	0.96	0.88	0.95
							Her2-enriched	0.88	0.95	0.66	0.99
							Basal	0.94	0.99	0.93	0.99
ROR risk classification	2370	0.84	(0.83, 0.86)	0.44	0.75	(0.73, 0.77)	Low	0.95	0.91	0.83	0.97
							Intermediate	0.50	0.95	0.73	0.86
							High	0.94	0.91	0.89	0.95
Binary ROR risk categorization (Bartlett)	2370	0.92	(0.91, 0.93)	0.56	0.84	(0.82, 0.87)	Low/Intermediate	0.91	0.94	0.95	0.89
							High	0.94	0.91	0.89	0.95

Supplemental Table 3. Selected SSP gene-rules for SSP models for clinical markers.

ER		PR		HER2		HER2 (ER+)		HER2 (ER-)		Ki67		NHG	
Gene rules	**Class**	**Gene rules**	**Class**	**Gene rules**	**Class**	**Gene rules**	**Class**	**Gene rules**	**Class**	**Gene rules**	**Class**	**Gene rules**	**Class**
LPIN1<ESR1	Positive	THAP2<PGR	Positive	ERBB2<ATP1A1	Negative	STARD3<BET1L	HER2nERp	ERBB2<PSMD8	HER2nERn	MYBL2<GPN2	Low	MYBL2<RILPL2	Grade 1
DISC1<CCDC170	Positive	LAD1<MAPT	Positive	MIEN1<SARS	Negative	GRB7<ZNF395	HER2nERp	MIEN1<TMEM147	HER2nERn	MKI67<ERCC6	Low	UBE2C<SIK3	Grade 1
PADI2<AGR3	Positive	GMIP<FGD3	Positive	PGAP3<WDTC1	Negative	MIEN1<CLSTN1	HER2nERp	PGAP3<DHX16	HER2nERn	TPX2<UTP14C	Low	BIRC5<PTPN21	Grade 1
ATP2C1<TBC1D9	Positive	PGR<THAP2	Negative	STARD3<CIZ1	Negative	PGAP3<WDTC1	HER2nERp	GRB7<RFXANK	HER2nERn	UBE2C<ALAD	Low	MYBL2<ZFYVE1	Grade 2
PSAT1<GREB1	Positive	MAPT<LAD1	Negative	GRB7<EHMT2	Negative	ERBB2<CD151	HER2nERp	STARD3<BABAM1	HER2nERn	PLK1<RIOX1	Low	CCNA2<METTL14	Grade 2
KHSRP<GATA3	Positive	FGD3<GMIP	Negative	TCAP<PSPN	Negative	GSDMB<CFAP69	HER2nERp	TCAP<KCNJ14	HER2nERn	PTTG1<CWC27	Low	AURKB<CTC1	Grade 2
INAVA<ANXA9	Positive			PSMD3<RAB13	Negative	MED1<PRKRA	HER2nERp	ORMDL3<ATP5L	HER2nERn	MELK<RAB33B	Low	ZFYVE1<MYBL2	Grade 3
GGCX<THSD4	Positive			CDK12<ASH1L	Negative	PSMD3<MRPL20	HER2nERp	PSMD8<ERBB2	HER2pERn	CCNB2<ZBTB44	Low	CIPC<TPX2	Grade 3
PPP1R14C<SERPINA11	Positive			ATP1A1<ERBB2	Positive	BET1L<STARD3	HER2pERp	TMEM147<MIEN1	HER2pERn	KIF4A<ZNF619	Low	APH1B<AURKA	Grade 3
PFKP<CA12	Positive			SARS<MIEN1	Positive	ZNF395<GRB7	HER2pERp	DHX16<PGAP3	HER2pERn	CDCA5<TMEM242	Low		
BEND3<C5AR2	Positive			WDTC1<PGAP3	Positive	CLSTN1<MIEN1	HER2pERp	RFXANK<GRB7	HER2pERn	CDCA8<FAM161B	Low		
FUT3<TTC6	Positive			CIZ1<STARD3	Positive	WDTC1<PGAP3	HER2pERp	BABAM1<STARD3	HER2pERn	MCM10<ZNF214	Low		
HAPLN3<SUSD3	Positive			EHMT2<GRB7	Positive	CD151<ERBB2	HER2pERp	KCNJ14<TCAP	HER2pERn	GPN2<MYBL2	High		
SLC15A2<ERBB4	Positive			PSPN<TCAP	Positive	CFAP69<GSDMB	HER2pERp	ATP5L<ORMDL3	HER2pERn	ERCC6<MKI67	High		
SRPK1<ARMT1	Positive			RAB13<PSMD3	Positive	PRKRA<MED1	HER2pERp			UTP14C<TPX2	High		
DSC2<NAT1	Positive			ASH1L<CDK12	Positive	MRPL20<PSMD3	HER2pERp			ALAD<UBE2C	High		
CCT8<SLC39A6	Positive									RIOX1<PLK1	High		
CDK6<CLSTN2	Positive									CWC27<PTTG1	High		
NUDT8<DEGS2	Positive									RAB33B<MELK	High		
ESR1<LPIN1	Negative									ZBTB44<CCNB2	High		
CCDC170<DISC1	Negative									ZNF619<KIF4A	High		
AGR3<PADI2	Negative									TMEM242<CDCA5	High		
TBC1D9<ATP2C1	Negative									FAM161B<CDCA8	High		
GREB1<PSAT1	Negative									ZNF214<MCM10	High		
GATA3<KHSRP	Negative												
ANXA9<INAVA	Negative												
THSD4<GGCX	Negative												
SERPINA11<PPP1R14C	Negative												
CA12<PFKP	Negative												
C5AR2<BEND3	Negative												
TTC6<FUT3	Negative												
SUSD3<HAPLN3	Negative												
ERBB4<SLC15A2	Negative												
ARMT1<SRPK1	Negative												
NAT1<DSC2	Negative												
SLC39A6<CCT8	Negative												
CLSTN2<CDK6	Negative												
DEGS2<NUDT8	Negative												

Supplemental Table 4. SSP performance validated against clinicopathological consensus data (re-stain and re-assessed) in the independent ABiM material from Brueffer et al. [24].

		Accuracy			Kappa						
SSP model	**n**	**Accuracy**	**95% CI**	**AccuracyNull**	**Kappa**	**95% CI**	**class value**	**Sensitivity**	**Specificity**	**Pos Pred Value**	**Neg Pred Value**
ER	405	0.97	(0.94, 0.98)	0.78	0.90	(0.85, 0.95)	Positive	0.96	0.98	0.99	0.88
PR	405	0.84	(0.80, 0.87)	0.66	0.67	(0.59, 0.74)	Positive	0.81	0.91	0.94	0.71
HER2	405	0.80	(0.76, 0.84)	0.79	0.55	(0.47, 0.63)	Positive	0.95	0.76	0.52	0.98
HER2 (SSP ER specific)	405	0.88	(0.85, 0.91)	0.79	0.69	(0.61, 0.77)	Positive	0.93	0.87	0.66	0.98
Ki67	405	0.67	(0.63, 0.72)	0.57	0.39	(0.32, 0.46)	High	0.98	0.44	0.57	0.97
							Grade 1	0.60	0.89	0.43	0.94
NHG	405	0.65	(0.60, 0.69)	0.47	0.41	(0.34, 0.48)	Grade 2	0.32	0.92	0.73	0.66
							Grade 3	0.95	0.60	0.68	0.93

Supplemental Table 5. SSP model vs. Prosigna model when evaluating identically sourced RNA and Prosigna model evaluation using fresh frozen tissue (FT) vs. FFPE material in the independent external clinical series ABiM.

ABiM		Accuracy		Kappa					
SSP model *vs.* Prosigna* FT	**n****	**Accuracy 95% CI**	**AccuracyNull**	**Kappa 95% CI**	**class value**	**Sensitivity**	**Specificity**	**Pos Pred Value**	**Neg Pred Value**
Subtype	100	0.87 (0.79, 0.93)	0.40	0.81 (0.72, 0.91)	Luminal A	0.91	0.94	0.89	0.95
					Luminal B	0.83	0.98	0.97	0.89
					Basal	0.81	1.00	1.00	0.97
					Her2-enriched	1.00	0.91	0.53	1.00
ROR risk classification	98	0.79 (0.69, 0.86)	0.58	0.61 (0.48, 0.74)	Low	0.73	0.90	0.58	0.95
					Intermediate	0.42	0.94	0.73	0.82
					High	0.96	0.78	0.86	0.94
Binary ROR risk categorization (Bartlett)	98	0.89 (0.81, 0.94)	0.58	0.76 (0.63, 0.89)	Low/Intermediate	0.78	0.96	0.94	0.86
					High	0.96	0.78	0.86	0.94

ABiM		Accuracy		Kappa					
Prosigna^ FT *vs.* FFPE	**n^^**	**Accuracy 95% CI**	**AccuracyNull**	**Kappa 95% CI**	**class value**	**Sensitivity**	**Specificity**	**Pos Pred Value**	**Neg Pred Value**
Subtype	100	0.82 (0.73, 0.89)	0.38	0.74 (0.63, 0.85)	Luminal A	0.79	0.92	0.86	0.88
					Luminal B	0.85	0.83	0.73	0.92
					Basal	1.00	0.98	0.88	1.00
					Her2-enriched	0.64	1.00	1.00	0.95
ROR risk classification	98	0.84 (0.75, 0.90)	0.60	0.71 (0.59, 0.84)	Low	0.70	0.99	0.93	0.93
					Intermediate	0.79	0.86	0.58	0.94
					High	0.90	0.90	0.93	0.85
Binary ROR risk categorization (Bartlett)	98	0.90 (0.82, 0.95)	0.60	0.79 (0.67, 0.91)	Low/Intermediate	0.90	0.90	0.85	0.93
					High	0.90	0.90	0.93	0.85

*Prosigna reference is Nanostring data (not clinical test) generated in Lund on **fresh tissue (FT)** and sent to Nanostring for readout of Prosigna classification results
**Prediction performance evaluated in ABiM (all available cases)
^Prosigna is Nanostring data (not clinical test) generated in Lund on **fresh tissue (FT) and FFPE** material and sent to Nanostring for readout of Prosigna classification results
^^Prediction performance evaluated in ABiM (all available cases)

Supplemental Table 6. Concordance analysis of emulated treatment recommendation between SSP and Prosigna for ER+ HER2- N0 cases in the external clinical series OSLO2-EMIT0 and ABiM.

OSLO2-EMIT0		Accuracy		Kappa					
SSP vs. Prosigna* FFPE	n	Accuracy 95% CI	AccuracyNull	Kappa 95% CI	class value	Sensitivity	Specificity	Pos Pred Value	Neg Pred Value
ETR	54	0.76 (0.62, 0.87)	0.54	0.61 (0.43, 0.80)	None	0.67	0.95	0.80	0.91
					Endo	0.72	0.80	0.81	0.71
					ChemoEndo	0.92	0.85	0.67	0.97
ETR dichotomized for chemotherapy	54	0.87 (0.75, 0.95)	0.76	0.69 (0.48, 0.90)	None/Endo	0.85	0.92	0.97	0.67
					ChemoEndo	0.92	0.85	0.67	0.97

*Reference is Prosigna clinical test on FFPE

ABiM		Accuracy		Kappa					
SSP vs. Prosigna** FFPE	n	Accuracy 95% CI	AccuracyNull	Kappa 95% CI	class value	Sensitivity	Specificity	Pos Pred Value	Neg Pred Value
ETR	33	0.82 (0.65, 0.93)	0.45	0.70 (0.48, 0.93)	None	1.00	1.00	1.00	1.00
					Endo	0.80	0.83	0.80	0.83
					ChemoEndo	0.77	0.85	0.77	0.85
ETR dichotomized for chemotherapy	33	0.82 (0.65, 0.93)	0.61	0.62 (0.34, 0.89)	None/Endo	0.85	0.77	0.85	0.77
					ChemoEndo	0.77	0.85	0.77	0.85

**Prosigna reference is Nanostring data (not clinical test) generated in Lund on FFPE material and sent to Nanostring for readout of Prosigna classification results

OSLO2-EMIT0 and ABiM		Accuracy		Kappa					
SSP vs. Prosigna*** FFPE	n	Accuracy 95% CI	AccuracyNull	Kappa 95% CI	class value	Sensitivity	Specificity	Pos Pred Value	Neg Pred Value
ETR	87	0.78 (0.68, 0.86)	0.51	0.65 (0.51, 0.79)	None	0.76	0.97	0.87	0.94
					Endo	0.75	0.81	0.80	0.76
					ChemoEndo	0.85	0.85	0.71	0.93
ETR dichotomized for chemotherapy	87	0.85 (0.77, 0.92)	0.70	0.66 (0.50, 0.83)	None/Endo	0.85	0.85	0.93	0.71
					ChemoEndo	0.85	0.85	0.71	0.93

***Prosigna results for OSLO2-EMIT0 cases are from the clinical test on FFPE material. Prosigna results for ABiM cases are from Nanostring data (not clinical test) generated in Lund on FFPE material and sent to Nanostring for readout of Prosigna classification results

Supplemental Figures 1-8

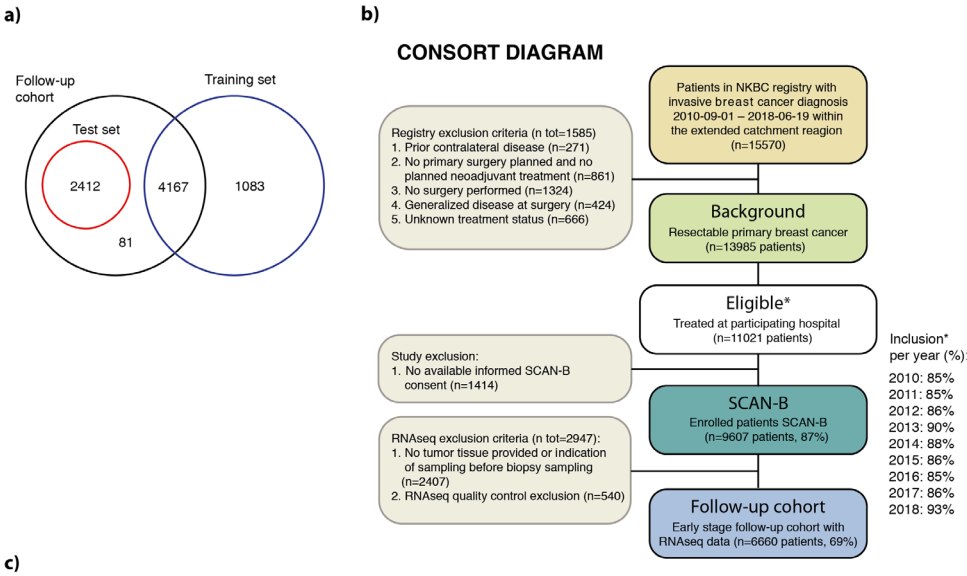

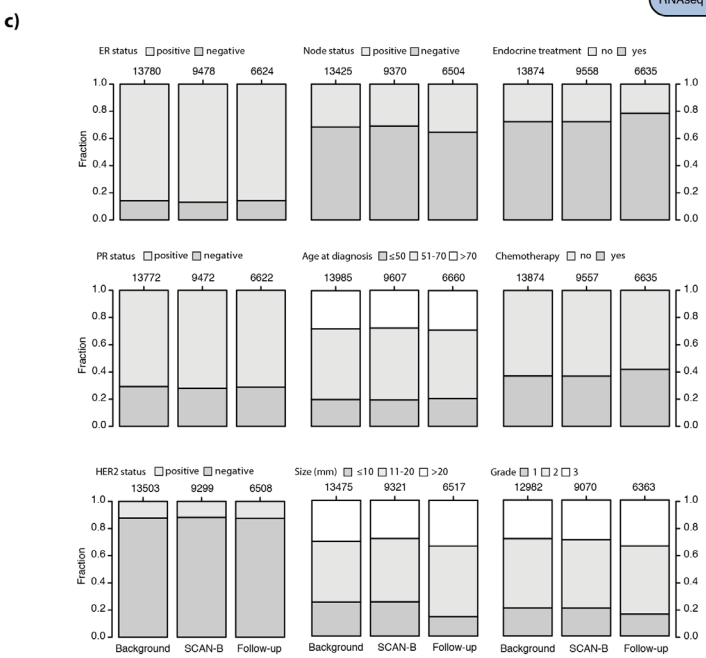

Supplemental Figure 1. Venn diagram of patient overlap in the SCAN-B study material cohorts and consort diagram of patient selection for the early-stage follow-up cohort with bar charts illustrating population-based representativeness compared to the background population. **(a)** Venn diagram of patient overlap for the follow-up cohort of early breast cancer (black), the training set (blue), and independent test set (red). **(b)** Consort diagram of patient inclusion in the follow-up cohort of early breast cancer. **(c)** Bar charts of incidence for important clinicopathological variables in the background population (left), enrolled SCAN-B patients (center), and SCAN-B patients with RNA-sequencing data (right) in the follow-up cohort. NKBC: Swedish national breast cancer quality registry.

*Statistics for eligible and yearly inclusion rates are restricted to participating hospitals and respective start date for enrollment. Original participating hospitals started enrollmed during the fall of 2010. Uppsala and Jönköping started enrollment in 2013 and 2015 respectively.

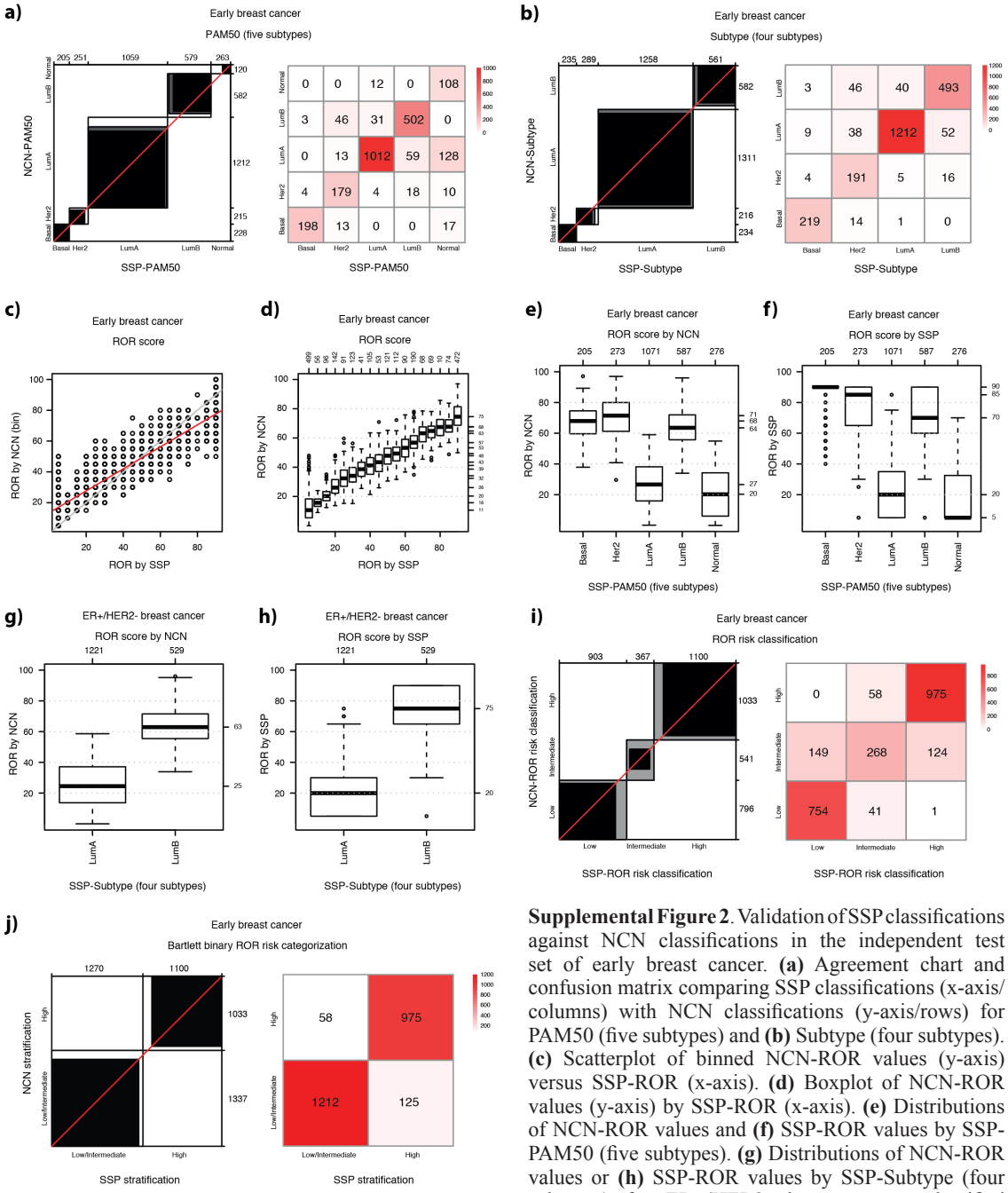

Supplemental Figure 2. Validation of SSP classifications against NCN classifications in the independent test set of early breast cancer. **(a)** Agreement chart and confusion matrix comparing SSP classifications (x-axis/columns) with NCN classifications (y-axis/rows) for PAM50 (five subtypes) and **(b)** Subtype (four subtypes). **(c)** Scatterplot of binned NCN-ROR values (y-axis) versus SSP-ROR (x-axis). **(d)** Boxplot of NCN-ROR values (y-axis) by SSP-ROR (x-axis). **(e)** Distributions of NCN-ROR values and **(f)** SSP-ROR values by SSP-PAM50 (five subtypes). **(g)** Distributions of NCN-ROR values or **(h)** SSP-ROR values by SSP-Subtype (four subtypes) for ER+/HER2- breast cancer classified as Luminal A or Luminal B. **(i)** Agreement chart and confusion matrix comparing SSP classification (x-axis/columns) with NCN classification (y-axis/rows) for ROR risk classification and **(j)** emulated treatment recommendation.

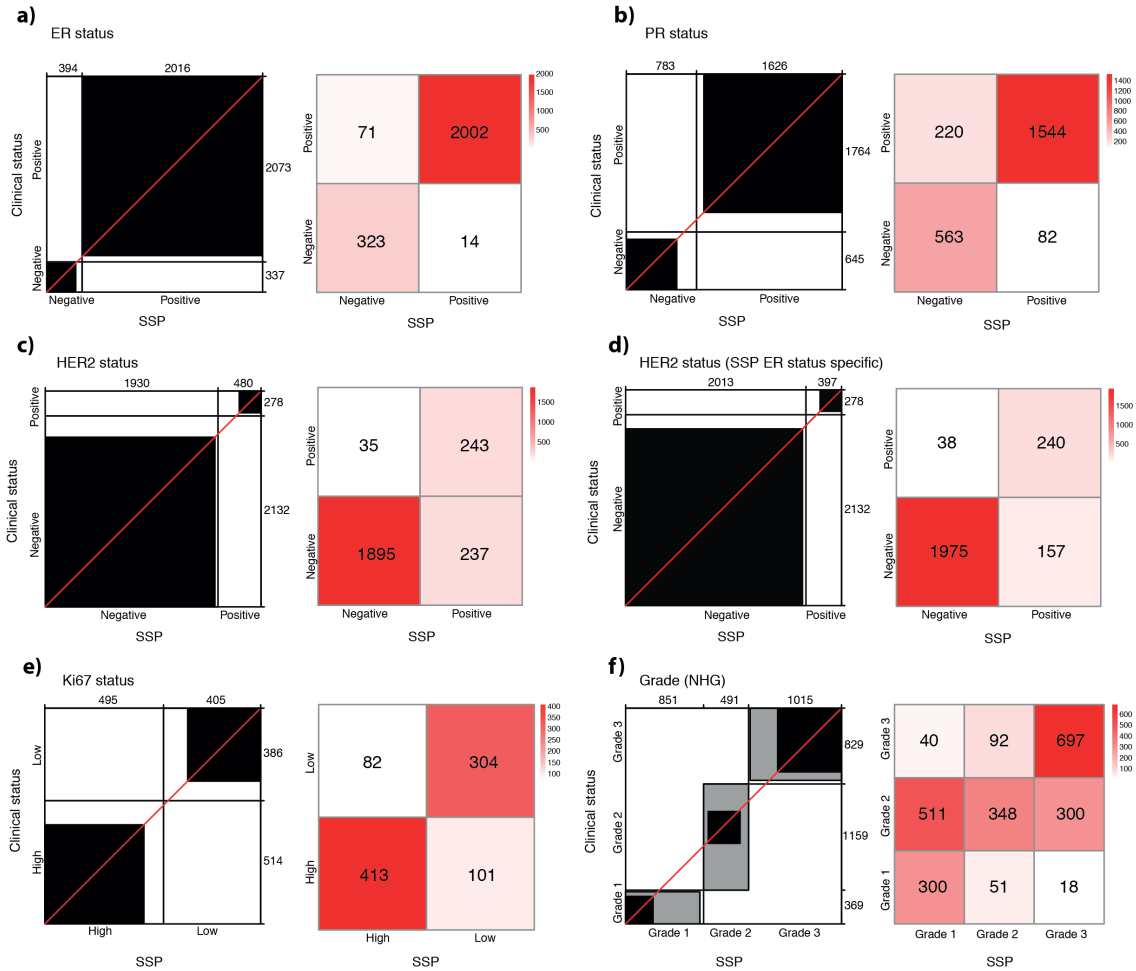

Supplemental Figure 3. Validation of SSP models for clinical markers in the independent population-based test set of early breast cancer. Agreement chart and confusion matrix comparing the SSP classifications (x-axis/columns) with clinical histopathology status (y-axis/rows) for **(a)** ER status, **(b)** PR status, **(c)** HER2 status using a general SSP model, **(d)** HER2 status using a SSP model specific for ER status, **(e)** Ki67-status, and **(f)** NHG.

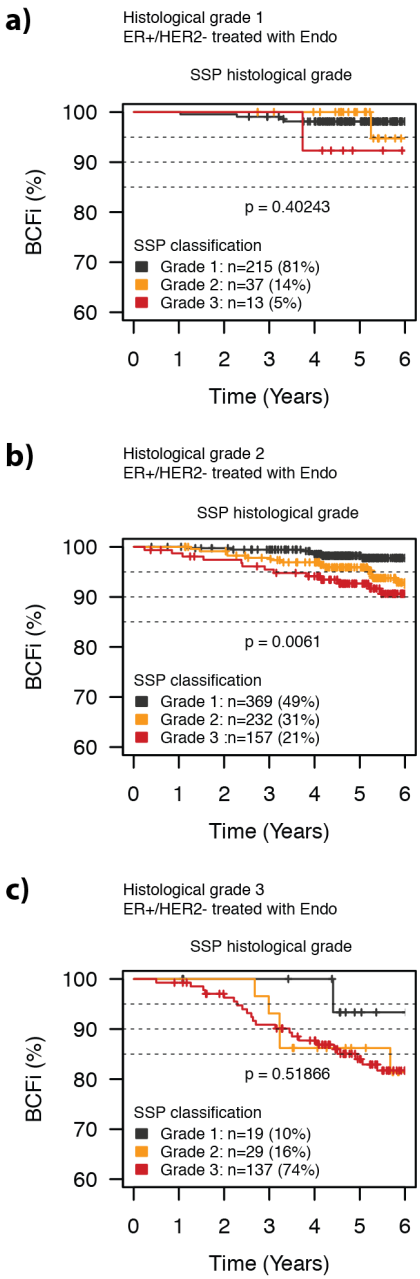

Supplemental Figure 4. Kaplan-Maier plot for SSP classification of NHG for groups of separate clinical NHG grade in patients diagnosed with ER+/HER2- breast cancer and that only received endocrine adjuvant treatment: **(a)** clinical NHG 1, **(b)** clinical NHG 2, **(c)** clinical NHG 3.

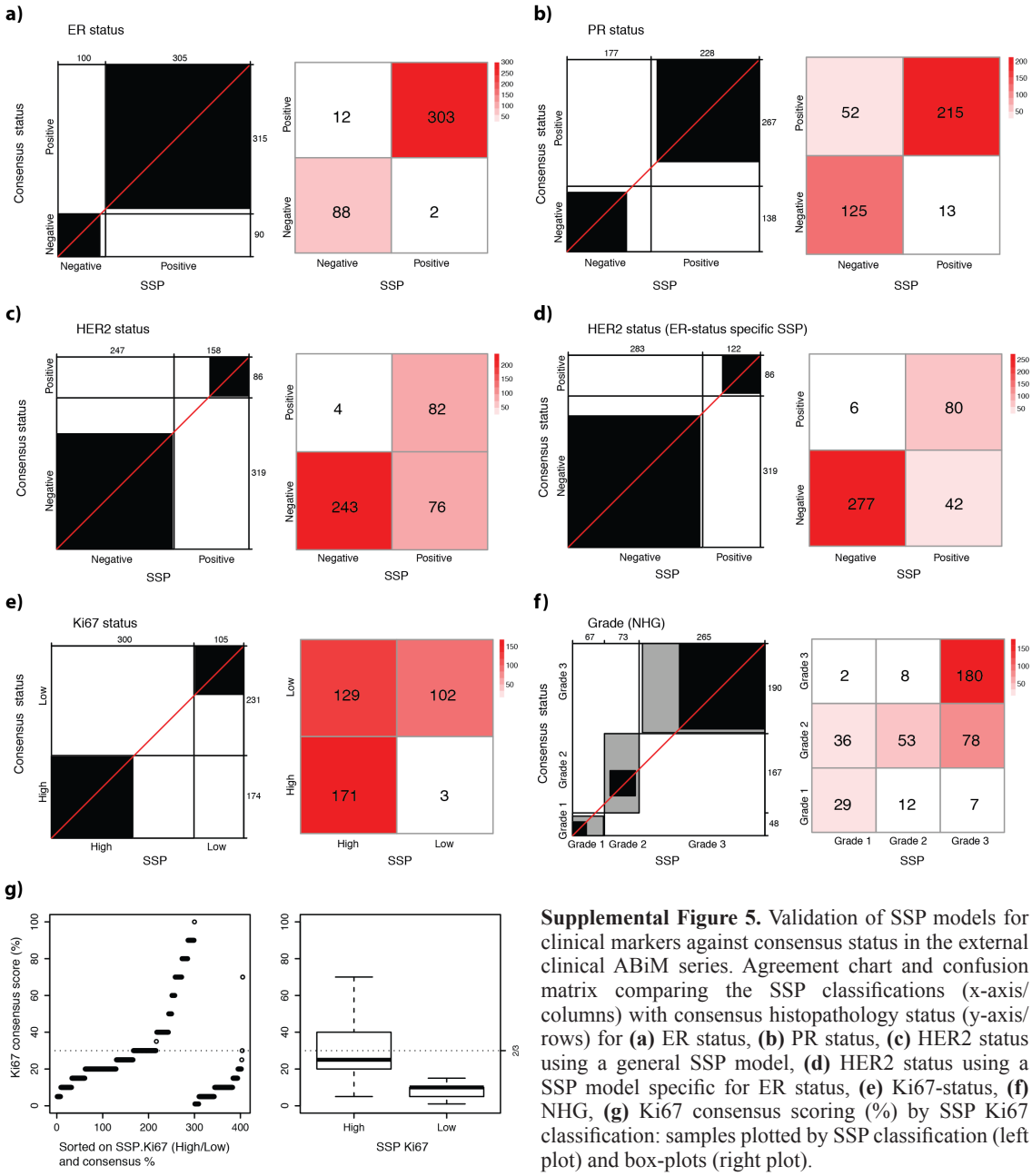

Supplemental Figure 5. Validation of SSP models for clinical markers against consensus status in the external clinical ABiM series. Agreement chart and confusion matrix comparing the SSP classifications (x-axis/columns) with consensus histopathology status (y-axis/rows) for **(a)** ER status, **(b)** PR status, **(c)** HER2 status using a general SSP model, **(d)** HER2 status using a SSP model specific for ER status, **(e)** Ki67-status, **(f)** NHG, **(g)** Ki67 consensus scoring (%) by SSP Ki67 classification: samples plotted by SSP classification (left plot) and box-plots (right plot).

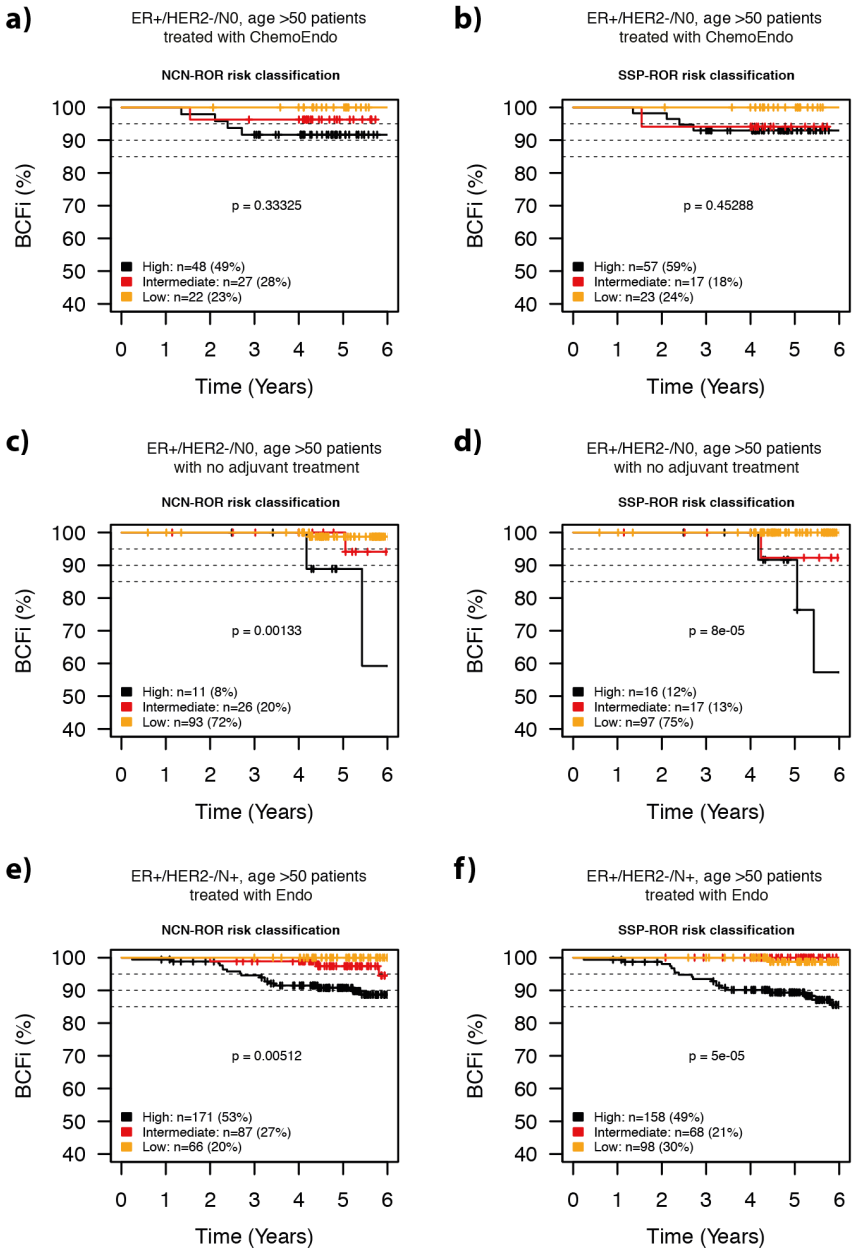

Supplemental Figure 6. Comparing SSP and NCN classifications in the independent population-based test set by assessment of prognostic value. **(a)** Kaplan-Meier plots for stratification by ROR risk classification from SSP-ROR risk category and **(b)** NCN-ROR risk category in ER+/HER2-/N0 disease diagnosed over 50 years of age treated with chemotherapy in addition to endocrine adjuvant treatment. **(c)** Kaplan-Meier plots for stratification by ROR risk classification from SSP-ROR risk category and **(d)** NCN-ROR risk category in ER+/HER2-/N0 disease diagnosed over 50 years of age that did not receive any adjuvant treatment. **(e)** Kaplan-Meier plots for stratification by ROR risk classification from SSP-ROR risk category and **(f)** NCN-ROR risk category in ER+/HER2-/N+ disease diagnosed over 50 years of age treated with endocrine adjuvant treatment alone.

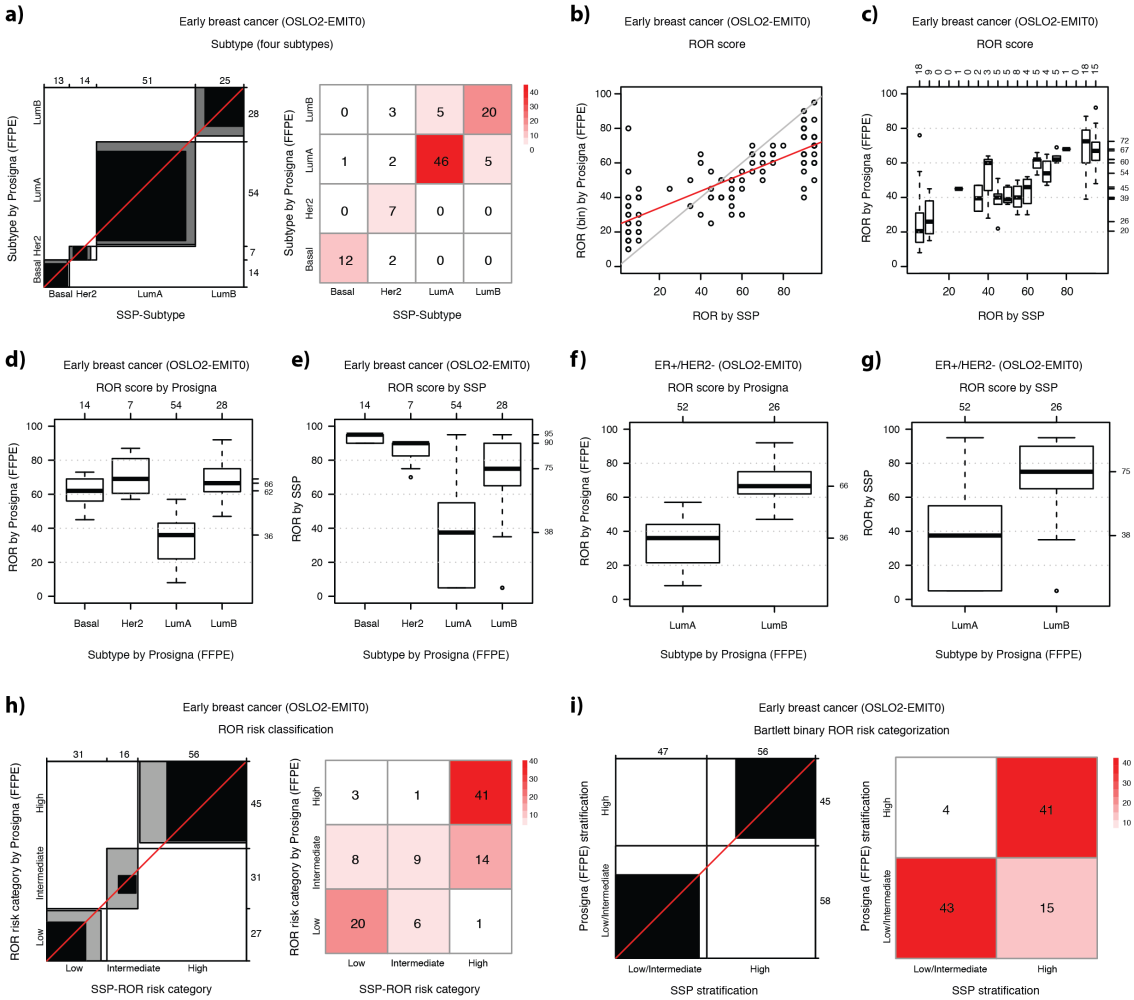

Supplemental Figure 7. Comparing SSP classifications from fresh frozen tissue against the clinical Prosigna test from FFPE tissue in an independent clinical series of primary breast cancer (OSLO2-EMIT0). **(a)** Agreement chart and confusion matrix comparing SSP classifications (x-axis/columns) with Prosigna classifications (y-axis/rows) for Subtype (four subtypes). **(b)** Scatterplot of binned Prosigna ROR values (y-axis) versus SSP-ROR (x-axis). **(c)** Boxplots of Prosigna ROR values (y-axis) by SSP-ROR (x-axis). **(d)** Distributions of Prosigna ROR values and **(e)** SSP-ROR values by Prosigna classification for Subtype (four subtypes). **(f)** Distributions of Prosigna ROR values and **(g)** SSP-ROR values by Prosigna classification for Subtype (four subtypes) for ER+/HER2- breast cancer classified as Luminal A or Luminal B. **(h)** Agreement chart and confusion matrix comparing SSP classification (x-axis/columns) with Prosigna classification (y-axis/rows) for ROR risk category and **(i)** the two-group ROR stratification according to Bartlett et al. [5].

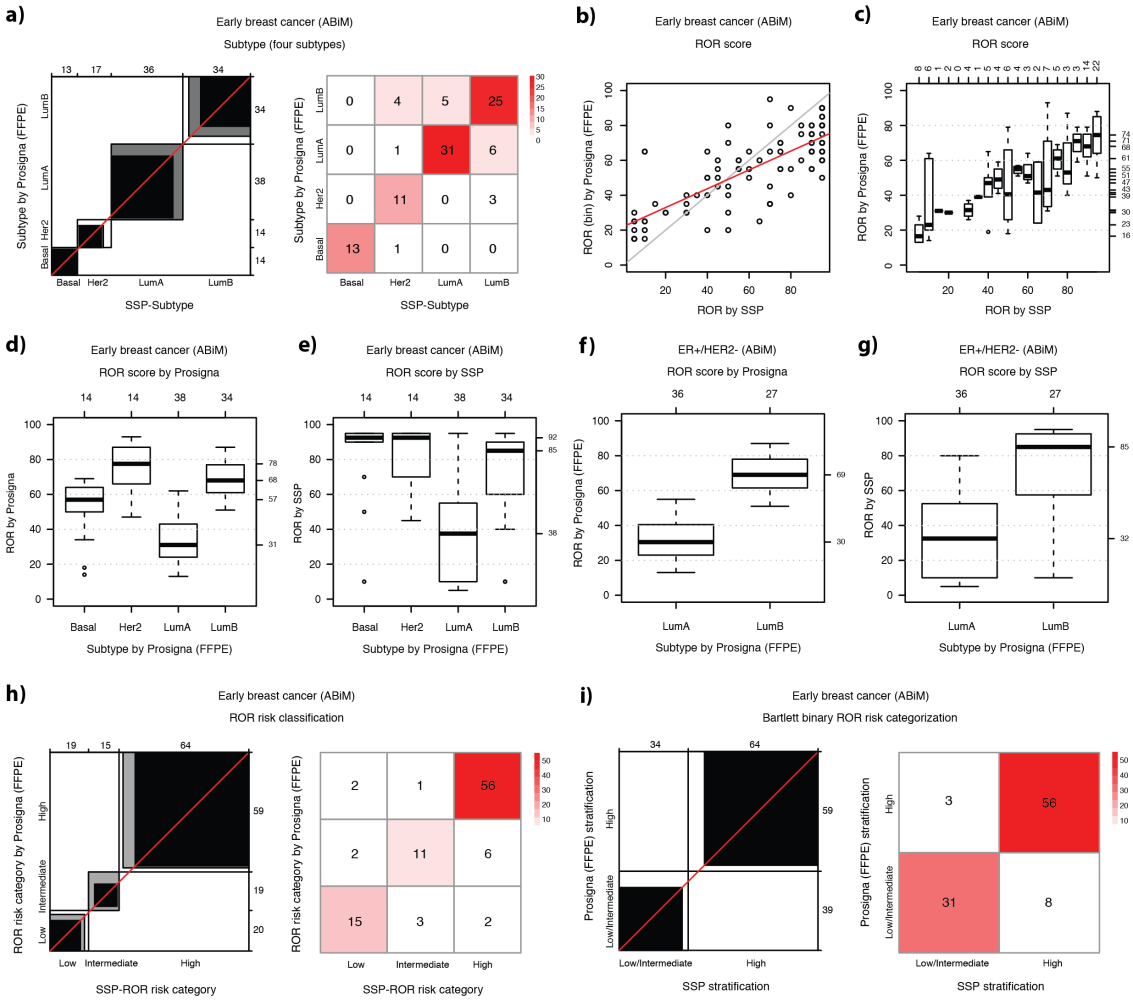

Supplemental Figure 8. Comparing SSP classifications from fresh frozen tissue against the Prosigna model on Nanostring data from FFPE tissue in an independent clinical series of early breast cancer (ABiM). **(a)** Agreement chart and confusion matrix comparing SSP classifications (x-axis/columns) with matched Prosigna classifications (y-axis/rows) for Subtype (four subtypes). **(b)** Scatterplot of binned Prosigna ROR values (y-axis) versus SSP-ROR (x-axis). **(c)** Boxplots of Prosigna ROR values (y-axis) by SSP-ROR (x-axis). **(d)** Distributions of Prosigna ROR values and **(e)** SSP-ROR values by Prosigna classification for Subtype (four subtypes). **(f)** Distributions of Prosigna ROR values and **(g)** SSP-ROR values by Prosigna classification for Subtype (four subtypes) for ER+/HER2- breast cancer classified as Luminal A or Luminal B. **(h)** Agreement chart and confusion matrix comparing SSP classification (x-axis/columns) with Prosigna classification (y-axis/rows) for ROR risk category and **(i)** the two-group ROR stratification according to Bartlett et al. [5].